Newly Synthesized Schiff Base Complexes with Selected Metals as Human Anti Breast Cancer MCF-7 Activity

Sohaib Gamal Ali[1], Abdou S. El-Tabl[2], Ahmed A. A.Shabana[1], Moshira M. Abd-El Wahed[3] , Ahmed M.Ashour[2],Mohammed H. H. Abu-Setta[*2] and Ahmed S. Elzaref[1]

[1] *Department of Chemistry, Faculty of Science, Al-Azhar University, Cairo, Egypt.*
[2] *Department of Chemistry, Faculty of Science, Menoufia University, Shebin El-Kom, Egypt.*
[3]*Department of Pathology, Faculty of Medicine, Menoufia University, Shebin El-Kom, Egypt.*

Abstract

Chemotherapeutic drugs have several major drawbacks. Therefore, motivation for developing novel drug complexes as anti-breast cancer agents with different mechanism of action has arisen. This study aimed to evaluate the influence of newly synthesized ligand namely N-(2-((2-hydroxybenzylidene)amino) phenyl)4(octyloxy) benzamide and its complexes with selected metals such as Cu(II), Zn(II), Ni(II), Co(II), Ca(II), Pb(II), Ba(II), Sr(II), Fe(III) and Cr(III) which were synthesized and showed a good yield. Investigations and characterizations of the ligand and its metal complexes to confirm there expected structure were carried out using elemental analyses such as IR, Mass spectroscopy, ^{1}HNMR, UV-Vis, ESR spectroscopy, thermal analysis (TGA and DTA), magnetic susceptibility and molar conductance measurements. The ligand and some of its metal complexes showed high biological activity and cytotoxicity against human breast cancer cell Lines MCF-7 (*invitro* study). The obtained results suggested that, some metal complexes could be considered as a potential anti-breast cancer agent with a higher efficacy than the standard drug (Cisplatin) and with low or no toxicity action observed against experimental animals (*invivo* studies).

Keywords: Metal complexes, Spectra, Magnetism, Cytotoxicity, Breast cancer.

1. Introduction

Development of a new chemotherapeutic Schiff bases and their metal complexes is now attracting the attention of medicinal chemists. Metals-based compounds were widely used in the treatment of diseases conditions, but the lack of clear distinction between the therapeutic and toxic doses was major challenge. With the discovery of cisplatin by Barnett Rosenberg in 1960, a milestone in the treatment of cancers was witnessed. Platinum drugs,

such as cisplatin carboplatin and oxaliplatin are the mainstay of the metal-based compound in the treatment of cancer, but the delay in the therapeutic accomplishment of other metal-based compounds hampered the progress of research in this filed [1]. Mononuclear Schiff-base copper(II) complexes were synthesized and characterized by X-ray crystallography [2]. The result showed that, all complexes demonstrated good cytotoxicity against cancer cell lines [2]. The anti-cancer activity of many forms of synthesized gold (I) complexes had been evaluated against cancer cell lines [3]. Therapeutic potentials of metal-based compound date back to ancient time, during this period, the ancient Assyrian, Egyptian and Chinese knew about the importance of using metal-based compounds in treatment of diseases, such as the use of cinnabar (mercury sulfide) in the treatment of aliments[4]. Cancer occurs in cells, comes from genetics harm, and is preventing control on the tissue. There are many types of cancer; breast cancer is one of the most common types of oncology. Breast cancer rate increase to fourfold in the world, rate range from 27 per 100,000 in middle Africa and eastern Asia 96 in Western Europe [5]. In USA, the percentage of breast cancer is 19% from women ages from 30 to 49 years and 44% from women ages 65 years or older [6]. In Africa countries, the breast cancer occurs in high percentage in older women [7]. In Arab populations, the breast cancer occurs from 2 to 3 women younger than 50 years old [8]. In Egypt, the rate of breast cancer is 30 per 100,000 of populations in ages from 30-35 years. Cells if untreated, the cancer is rapidly dividing and spreading in all areas of the body, chemotherapeutics agent used in tumors treatment by prevent of tumor cell from grow abnormally and dividing according to stopping the cancer from spreading and kill it. In chemotherapy, there is the important issue is killing the tumor cells without damage the healthy cells, the transition metal is effective inhibitors of DNA, the main system of molecular biology is deoxyribose nucleic acid (DNA) and transfer to ribonucleic acid (RNA) to protein synthesis [9]. Schiff bases are main and great ways due to their applications in wide fields. Schiff base ligands and there metal complexes are usually used for different biological activity like antitumor, antimicrobial, anti-inflammatory, antifungal and antibacterial activity. The concept of selective targeting remains the hope of the future in developing therapeutics that would selective target cancer cells and leave healthy cells unharmed. This paper outlines recent compounds as anti-breast cancer agents.

2. Experimental

2.1. Materials

All chemicals and Solvents used in synthesis of ligand and preparation its metals complexes were of the analytical grade and high purity. Sodium-4-(methoxycarbonyl)phenolate was obtained from Sigma-Aldrich (assay ≥ 99%), 1-Bromo-octane was obtained from Sigma-Aldrich (assay ≥ 98%), o-phenylenediamine was obtained from Sigma-Aldrich (assay ≥ 99%), Salicylaldehyde was obtained from MERCK-Schuchardt (assay ≥ 99.9%) and absolute ethanol was obtained from Sigma-Aldrich (assay ≥ 99.7%). The following chemicals used in preparation of metal complexes were obtained from Sigma-Aldrich: $Cu(OAc)_2.H_2O$ (assay ≥ 99.9%), $Mn(OAc)_2.4H_2O$ (assay ≥ 99.9%), $Zn(OAc)_2.2H_2O$ (assay ≥ 99.9%), $Ni(OAc)_2.4H_2O$ (assay ≥ 99.9%), $Pb(OAc)_2.3H_2O$ (assay ≥ 99.9%), $Cu(SO_4)_2.5H_2O$ (assay ≥ 99.9%), $Ni(SO_4)_2.6H_2O$ (assay ≥ 99.9%), $CoSO_4$ (assay ≥ 99.9%), $Fe_2(SO_4)_3$ (assay ≥ 99.9%), $Cr_2(SO_4)_3.18H_2O$ (assay ≥ 99.9%), $Mg(SO_4).7H_2O$ (assay ≥ 99.9%), $CuCl_2.2H_2O$ (assay ≥ 99.9%), $CoCl_2.6H_2O$ (assay ≥ 99.9%), $BaCl_2.2H_2O$ (assay ≥99.9%), $SrCl_2.6H_2O$ (assay ≥ 99.9%), $CuCO_3.Cu(OH)_2$ (assay≥99.9%), BiOCl (assay≥99.9%), $(Ca(OH)_2$ (assay≥99.9%).

2.2. Synthesis of the ligand

The ligand**,** (H_2L) **(1)** was prepared by addition of 1-bromo-octane (2.7 g, 1.0 mol) dissolved in 20 ml ethanol to sodium-4-(methoxycarbonyl) phenolate (2.0 g, 1.0mol) dissolved in 20 ml of ethanol solution. The mixture was refluxed with stirring for 3 hours and then left to cool at room temperature. The formed methyl-4-(octyloxy) benzoate precipitate was filtered off then left it to dry at room temperature [product (1)]. O-phenylenediamine (1.24 g, 1.0 mol) dissolved in 20 ml in ethanol was added to the formed product (1) of methyl-4-(octyloxy) benzoate. The mixture was refluxed with stirring for 2 hours and then left to cool at room temperature to give N-(2-aminophenyl)-4-(octyloxy) benzamide [product (2)]. Finally, salicylaldehyde (1.36 g, 1.0 mol) dissolved in 20 ml ethanol was added to N-(2-aminophenyl)-4-(octyloxy) benzamide product (2). The mixture was refluxed and stirring for 3 hours at 100ºC, then left to cool at room temperature. The solid product which formed was filtered off and washed it with cold ethanol then dried in desiccator under vacuum over anhydrous $CaCl_2$, to give ligand **(1)**.

2.3. Preparation of metal complexes (2)-(19)

Synthesis of complexes **(2)-(19)** as (1L:1M) molar ratio was carried out by refluxing a hot ethanolic solution of ligand **(1)** (1.0 g, 1.0 mol) (30 ml) with a hot ethanolic solution of metal salts of (0.44 g, 1.0 mol) (30 ml) of $Cu(OAc)_2.H_2O$, complex **(2)**, (0.55 g, 1.0 mol) of $Mn(OAc)_2.4H_2O$, complex **(3)**, (0.49 g, 1.0 mol) of $Zn(OAc)_2.2H_2O$, complex **(4)**, (0.56 g, 1.0 mol) of $Ni(OAc)_2.4H_2O$, complex **(5)**, (0.85 g, 1.0 mol) of $Pb(OAc)_2.3H_2O$, complex **(6)**, (0.56 g, 1.0 mol) of $Cu(SO_4)_2.5H_2O$, complex **(7)**, (0.59 g, 1.0 mol) of $Ni(SO_4)_2.6H_2O$, complex **(8)**, (0.34 g, 1.0mol) of $CoSO_4.3H_2O$, complex **(9)**, (0.90g,1.0mol) of $Fe_2(SO_4)_3.3H_2O$, complex **(10)**, (1.61 g, 1.0 mol) of $Cr_2(SO_4)_3.18H_2O$, complex **(11)**, (0.55 g, 1.0 mol) of $Mg(SO_4).7H_2O$, complex **(12)**, (0.30 g, 1.0 mol) of $CuCl_2.2H_2O$, complex **(13)**, (0.53 g, 1.0 mol) of $CoCl_2.6H_2O$, complex**(14)**, (0.55 g, 1.0 mol) of $BaCl_2.2H_2O$, complex **(15)**, (0.60 g, 1.0 mol) of $SrCl_2.6H_2O$, complex **(16)**, (0.49g,1.0mol) of $CuCO_3.Cu(OH)_2$, complex **(17)**, (0.58 g, 1.0 mol) of BiOCl, complex **(18)**, (0.16 g, 1.0 mol) of $Ca(OH)_2$, complex **(19).** The reaction mixtures were refluxed with stirring for 2-3 hours range, depending on the nature of the metal ion and the anion. The formed precipitates were filtrated off then dried in desiccator under vacuum over anhydrous $CaCl_2$, to give the corresponding complexes [Figure (1)].

2.4. Instrumentation and measurements

The ligand and its metal complexes were analyzed for C, H, N and Cl at the Micro Analytical Center, Cairo University, Egypt. Standard analytical methods were used to determine the metal ion content [10]. IR spectra of the ligand and its metal complexes were measured with KBr discs technique using a Jasco FT/IR 300E Fourier transform infrared spectrophotometer covering the range 400-4000 cm^{-1} [11]. The mass spectra of the ligand and some of its metal complexes were recorded on Shimadzu Qp-2010 plus mass spectrometer. ^{1}H-NMR spectra were obtained on Mercury-300 BB 300 MHz spectrometer [12]. Chemical shifts (ppm) were reported relative to TMS. The ESR spectra of solid complexes at room temperature were recorded using a Varian E-109 spectrophotometer; DPPH was used as a standard material [13]. The equation used to determine g- values was $g = (g_{DPPH})(H_{DPPH}) / H$ where: g_{DPPH} = 2.0036, H_{DPPH} = magnetic field of DPPH in gauss H = magnetic field of the sample in gauss [14]. The thermal analyses (DTA and TGA) were carried out on a Shimadzu DTG-60H thermal analyzer from room temperature to 700 ºC at

a heating rate of 10ºC/min. Electronic spectra in the 200-900 nm regions was recorded on a Perkin-Elmer 550 spectrophotometer. Magnetic susceptibilities were measured at 25ºC by using Sherwood Scientific magnetic balance, Cambridge science [15]. The magnetic moments were calculated from the equation

$$\textbf{Magnetic susceptibility: } (X_g) = CL(R-R_o)/10^9 \qquad (1)$$

Where

C: calibration constant for the instrument=2.086

L: length of sample in the tube

R: balance reading of the sample in the tube

M: mass in gram.

The molar conductances of 10^{-3} M DMSO solution of the complexes were measured at 25ºC with a Bibby conductometer type MCl. The resistance measured in ohms and the molar conductivities were calculated according to the equation

$$\Lambda_M = \frac{V \times K \times g}{Mw * \Omega} \qquad (2)$$

Where

Λ_M= molar conductivity / Ω^{-1} cm^2 mol^{-1}, V= volume of the complex solution/ ml, K= cell constant (0.92/ cm^{-1}), Mw= molecular weight of the complex, g= weight of the complex in gram and Ω= resistance.

The TLC of all compounds confirmed their purity [16].

2.5. Biological activity

2.5.1. *In vitro* studies

Evaluation of the cytotoxic activity of the ligand and some of its metal complexes was carried out in the Pathology Laboratory, Pathology Department, Faculty of Medicine, Menoufia University, Egypt. The evaluation process was carried out in vitro using the Sulfo- Rhodamine-Bstain (SRB) assay published method. Cells were plated in 96-multiwell plate (104 cells/well) for 24 hrs. Before treatment with the complexes to allow attachment of cell to the wall of the plate. Different concentrations of the compounds under test in DMSO (0, 5, 12.5, 25 and 50 µg/ml) were added to the cell monolayer, triplicate wells being prepared for each individual dose. Monolayer cells were incubated with the complexes for 48 hrs.at 37°C and using 5% CO2. After 48 hrs. Cells were fixed, washed and stained with Sulfo-Rhodamine-B-stain. Excess stain was washed with acetic acid and attached stain was

recovered with Tris EDTA buffer. Color intensity was measured in an ELISA reader. The relation between surviving fraction and drug concentration is plotted to get the survival curve for each tumor cell line after addition the specified compound [17].

2.5.2. In vivo studies

2.5.2.1.Toxicity study

Toxicity study of copper (II) complex **(2)** & nickel (II) complex **(5)** with molecular weights of complexes 661.77 and 638.93 and chemical formula $C_{32}H_{42}CuN_2O_9$ and $C_{32}H_{40}N_2NiO_8$ respectively was done. The complexes were dissolved in DMSO diluted by sterile saline 0.9 % NaCl in a maximum concentration of 0.2% by volume in order to be able to injected intra peritoneal.

2.5.2.2. Animals

Fifty healthy male albino rats 8 weeks old (180 - 200 g) were purchased from National Cancer Institute, Cairo, Egypt. Rats were housed in cages at regulated temperature (22- 25 °C). They were kept under good ventilation under a photoperiod of 12hr light/12hr darkness schedule with lights-on from 06:00 to 18:00. They all received a standard laboratory diet (60% ground corn meal, 10% bran, 15% ground beans, 10% corn oil, 3% casein, 1% mineral mixture and 1% vitamins mixture), purchased from Meladco Feed Company (Obour City, Cairo, Egypt) and supplied with water ad libitum throughout the experimental period.

2.5.2.2. Acute toxicity study

Determination of lethal dose 50 (LD_{50}) using experimental animals. In screening drugs, determination of LD_{50} is usually an initial step in the assessment and evaluation of the toxic characteristics of a substance. The LD_{50} of the studied compounds was determined as described by Akhila et al [17]. The acute intra-peritoneal toxicity of the chosen complexes was done on 20 animals (10 per group). The complxes were dissolved in DMSO diluted by sterile saline 0.9% NaCl in a maximum concentration of 0.2% by volume to be able to injected intraperitoneal. The chosen complexes were administrated with graded doses of 1×10^{-6}, 5×10^{-6}, 1×10^{-5} and reached to 1×10^{-4} mmole/L/Kg body weight under the same environmental conditions. After administration of the chosen complexes concentrations, the rats were observed for toxic effects after 24h of treatment. The toxicological effects were observed in terms of

mortality and expressed as lethal dose 50 (LD_{50}). The LD_{50} value of the complexes was determined. The LD_{50} for all tested complexes nanoparticles were devoid of any toxicity in rats when given the selected different doses by intra-peritoneal route [17].

2.5.2.3. Experimental design

Thirty animals were allowed 10 days for adaptation. They were then randomly distributed into 3 equal groups, 10 rats each. The animal groups were recognized as follows:

Group 1 (Control): Normal healthy control animals.

Group 2: Each animal was injected intra peritoneal with 1x10-5mmole/L of complex (1) for 6weeks.

Group 3: Each animal was injected intra peritoneal with 1x10-5mmole/L of complex (2) for 6weeks.

2.5.2.4. Blood collection

At the end of the experimental period (6 weeks), blood samples were collected from overnight rats, centrifuged at 3000 rpm for 10 min and the separated sera were frozen at -20 °C for future biochemical analysis.

2.5.2.5. Biochemical analyses

Liver enzymes activities, aspartate aminotransferase (AST) and alanine aminotransferase (ALT) were estimated using kinetic kits purchased by Human Diagnostic Kits, Germany [18]. The liver function, albumin concentration and kidney functions, blood urea and serum creatinine were measured using Diamond Diagnostic kits, Egypt. All biochemical analysis were determined using a Biosystems BTS-310 Spectrophotometer [19].

2.5.2.6. Hematological analyses

Determination of hemoglobin (Hb) using Drabkin's solution16, red blood corpuscles count (RBCs), total leucocytic count (TLC) and platelets count (PLTs) were determined manually [20, 21].

2.5.2.7. Statistical analysis

Data were subjected to statistical significance tests using one-way analysis of variance (ANOVA), followed by Duncan's multiple range test. The statistical analysis was carried out using SPSS 16.00 software. The results were

expressed as mean ± SE and the differences were considered significant at $P \leq 0.05$ [22].

3. Results and discussion

Metal complexes are colored, crystalline solids, non-hygroscopic, and showed stability at air and room temperature and moisture without decomposition for a long time > one year. The complexes are insoluble in water, methanol, ethanol, benzene, toluene, chloroform, acetonitrile but soluble in both (DMF) and (DMSO). The analytical, physical properties and spectral data for the ligand and its metal complexes presented in table **(1)**. Tables **(2)-(4)** confirmed the expected structures for Figures **(1).** The elemental spectral analysis indicated that, all complexes were formed by 1L: 1M molar ratio**.**

3.1. Conductance measurements

$1x10^{-3}$ molar solutions of the ligand and its metal complexes in DMSO were used for molar conductivities measurements. The ligand and its metal complexes showed low molar conductivities values, Table **(1**), confirming that, both the ligand and its metal complexes are non-electrolytic in nature, which confirmed coordination of the anions to the metal ions [23].

Table (1):-Analytical and physical data of the ligand [H_3L] and its metal complexes.

NO.	Ligands/Complexes	Color	FW	M.P (^oC)	Yield (%)	Calc. (Found) (%)				Molar Conductivity*
						C	H	N	M	
1.	$[H_2L]$ $C_{28}H_{32}N_2O_3$	Blackish brown	444.25	>300	93.4	75.70 (76.91)	7.20 (6.57)	6.30 (6.34)	-	2.31
2.	$[H_2L$ $Cu(OAc)_2.H_2O]H_2O$ $C_{32}H_{42}CuN_2O_9$	Dark black	661.77	>290	86.3	58.07 (57.29)	6.35 (6.40)	4.23 (4.21)	9.60 (9.79)	5.71
3.	$[H_2LMn(OAc)_2.H_2O]3$ H_2O $C_{32}H_{46}MnN_2O_{11}$	Dark black	689.14	>300	83.7	55.77 (57.71)	6.67 (6.66)	4.06 (4.00)	7.97 (8.01)	6.37
4.	$[H_2L$ $Zn(OAc)_2.H_2O]$ H_2O $C_{32}H_{42}N_2O_9Zn$	Dark brown	663.61	>300	89.1	57.91 (59.02)	6.33 (6.27)	4.22 (4.20)	9.85 (9.78)	4.78
5.	$[H_2L$ $Ni(OAc)_2.H_2O]$ $C_{32}H_{40}N_2NiO_8$	Yellowish Brown	638.93	>300	88.6	60.15 (59.75)	6.26 (5.59)	4.38 (4.35)	9.19 (9.09)	6.21

6.	$[H_2L$ $Pb(OAc)_2.H_2O]H_2O$ $C_{32}H_{42}N_2O_9Pb$	Black	805.43	>300	84.6	47.72 (48.10)	5.21 (5.20)	3.48 (3.50)	25.73 (25.79)	5.01
7.	$[H_2L$ $CuSO_4.2H_2O]H_2O$ $C_{28}H_{38}Cu\ N_2O_{10}S$	Brownish black	657.78	>300	78.9	51.12 (51.03)	5.78 (5.90)	4.26 (4.30)	9.66 (9.72)	6.23
8.	$[H_2L$ $NiSO_4.2H_2O]5H_2O$ $C_{28}H_{46}N_2NiO_{14}S$	Dark black	724.89	>300	77.4	46.39 (46.40)	6.35 (6.20)	3.86 (3.80)	8.10 (8.15)	6.12
9.	$[H_2LCoSO_4.2H_2O]3H_2O$ $C_{28}H_{42}CoN_2O_{12}S$	Black	689.15	>300	69.2	48.80 (48.90)	6.09 (6.10)	4.06 (4.20)	8.55 (8.60)	7.13
10.	$[HL$ $Fe(SO_4).2H_2O]2H_2O$ $C_{28}H_{39}FeN_2O_{11}S$	Dark brown	667.11	>300	81.3	56.41 (56.50)	5.37 (5.35)	4.70 (4.65)	9.37 (9.30)	6.82
11.	$[HL$ $CrSO_4.2H_2O]2H_2O$ $C_{28}H_{39}Cr\ N_2O_{11}S$	Dark black	663.24	>300	74.5	53.53 (53.60)	5.73 (5.70)	4.46 (4.45)	8.28 (8.30)	7.21
12.	$[H_2L$ $MgSO_4.2H_2O]5H_2O$ $C_{28}H_{46}MgN_2O_{14}S$	Dark brown	690.5	>300	76.1	48.70 (48.75)	6.66 (6.60)	4.06 (4.01)	3.52 (3.50)	6.92
13.	$[H_2L\ CuCl_2.H_2O]H_2O$ $C_{28}H_{36}CuCl_2N_2O_5$	Black	614.67	>300	82.7	54.71 (54.75)	5.86 (5.79)	4.56 (4.50)	10.34 (10.3)	6.13
14.	$[H_2L$ $CoCl_2.H_2O]2H_2O$ $C_{28}H_{38}CoCl_2N_2O_6$	Black	628.05	>300	62.4	53.54 (53.60)	6.05 (6.10)	4.46 (4.40)	9.38 (9.40)	6.23
15.	$[H_2L$ $BaCl_2.H_2O]3H_2O$ $C_{28}H_{40}BaCl_2N_2O_7$	Black	724.44	>300	65.3	46.42 (46.45)	5.52 (5.50)	3.87 (3.90)	18.96 (18.90)	5.98
16.	$[H_2L\ SrCl_2.H_2O]H_2O$ $C_{28}H_{36}Cl_2N_2O_5Sr$	Black	638.62	>300	70.2	64.24 (64.30)	6.11 (6.50)	5.35 (5.30)	8.37 (8.40)	5.23
17.	$[H_2L$ $CuCO_3.2H_2O]2H_2O$ $C_{29}H_{40}CuN_2O_{10}$	Brown	639.73	>300	86.9	54.44 (54.50)	6.25 (6.20)	4.38 (4.35)	9.93 (9.95)	4.34
18.	$[H_2L\ BiOCl]2H_2O$ $C_{28}H_{36}BiClN_2O_6$	Dark black	740.6	>300	82.4	43.36 (43.40)	4.86 (4.80)	3.78 (3.80)	28.20 (28.15)	3.57
19.	**[**H_2L $Ca(OH)_2.H_2O]2H_2O$ $C_{28}H_{40}CaN_2O_8$	Brown	572.27	>300	80.7	58.76 (58.80)	6.99 (6.85)	4.89 (4.75)	7.00 (7.10)	5.15

***$\Omega^{-1}cm^2mol^{-1}$**

3.2. Mass spectra

Mass spectrometry was used to confirm the molecular ion peaks of the ligand and some of its metal complexes and to investigate the fragment species [24]. The recorded mass spectrum for the ligand, table (2-a) revealed molecular

ion peak confirmed strongly the expected formula [25]. It showed a molecular ion peak at *m/z* 444.0 amu, confirming its formula weight (F.W. 444.0) and also the purity of the ligand prepared. The prominent mass fragmentation peaks observed at m/z = 52, 65, 77, 93, 121, 138, 152, 181, 207, 210, 237, 251, 264, 279, 293, 305, 321, 345, 409 and 444 amu corresponding to C_4H_4, C_5H_5,C_6H_5,C_6H_5O,C_8H_9O,$C_9H_{14}O$,$C_{10}H_{16}O$,$C_{11}H_{17}O_2$,$C_{12}H_{17}NO_2$, $C_{12}H_{20}NO_2$, $C_{14}H_{23}NO_2$, $C_{14}H_{23}N_2O_2$,$C_{15}H_{24}N_2O_2$,$C_{16}H_{27}N_2$,$C_{17}H_{29}N_2O_2$,$C_{18}H_{29}N_2O_2$, $C_{18}H_{29}N_2O_3$,$C_{20}H_{29}N_2O_3$,$C_{25}H_{32}N_2O_3$ and $C_{28}H_{32}N_2O_3$ moieties respectively, supported the expected structure for the ligand (Table 2-a). However, The mass spectrum for the $[H_2L\ Zn(OAc)_2H_2O].H_2O$ complex **(4)** (Table 2-b) showed the molecular ion peak at *m/*z 663 amu, confirming its formula weight (F.W. 663). The mass fragmentation pattern observed at *m/z* = 55, 77, 91, 121, 152, 156, 181, 182, 210, 224, 250, 288, 313, 349, 537, 552, 566 and 663 amu corresponding to C_4H_7, C_6H_{17}, C_6H_{19}, $C_7H_{21}O$, $C_8H_{24}O_2$, $C_8H_{28}O_2$,$C_{10}H_{29}O_2$, $C_{10}H_{30}O_2$, $C_{11}H_{32}NO_2$, $C_{12}H_{34}NO_2$, $C_{14}H_{36}NO_2$, $C_{16}H_{36}N_2O_2$, $C_{18}H_{37}N_2O_2$, $C_{21}H_{37}N_2O_2$, $C_{30}H_{37}N_2O_7$, $C_{31}H_{40}N_2O_7$, $C_{32}H_{42}N_2O_7$ and $C_{32}H_{42}N_2O_9Zn$ moieties respectively, conformed the expected structure for the complex (Table 2-b). However the mass spectrum for the $[H_2L\ CuCO_3.2H_2O]2H_2O$ complex **(17)** (Table 2-c) showed the molecular ion peak at *m/*z 625 amu, confirming its formula weight (F.W. 639).The mass fragmentation patterns observed at *m/z* = 55, 57, 71, 91, 120, 146, 182, 210, 237, 239, 256, 281, 313, 339, 354, 368, 396, 452, 465, 479, 524, 552, 564, 576 and 639 amu correspond to C_4H_7, C_4H_9, C_5H_{11}, C_6H_{19}, C_8H_{23}, $C_{10}H_{26}$, $C_{13}H_{26}$, $C_{14}H_{26}O$, $C_{15}H_{27}NO$, $C_{15}H_{29}NO$, $C_{15}H_{30}NO_2$, $C_{17}H_{31}NO_2$, $C_{17}H_{31}NO_4$, $C_{19}H_{33}NO_4$, $C_{20}H_{36}NO_4$, $C_{20}H_{36}N_2O_4$, $C_{21}H_{36}N_2O_5$, $C_{23}H_{36}N_2O_7$, $C_{24}H_{37}N_2O_7$, $C_{25}H_{39}N_2O_7$, $C_{26}H_{40}N_2O_9$, $C_{27}H_{40}N_2O_{10}$, $C_{28}H_{40}N_2O_{10}$, $C_{29}H_{40}N_2O_{10}$ and $C_{29}H_{40}CuN_2O_{10}$ moieties respectively, conformed the expected structure of the complex.

Table (2-a): Mass spectrum the ligand $[H_2L]$

m/z	*Rel. Int.*	*Assignments*
52	24.0	C_4H_4
65	23.0	C_5H_5
77	24.0	C_6H_5
93	17.0	C_6H_5O
121	100.0	C_8H_9O

138	23.0	$C_9H_{14}O$
152	53.0	$C_{10}H_{16}O$
181	23.0	$C_{11}H_{17}O_2$
207	32.0	$C_{12}H_{17}NO_2$
210	40.0	$C_{12}H_{20}NO_2$
237	26.0	$C_{14}H_{23}NO_2$
251	24.0	$C_{15}H_{23}N_2O_2$
264	18.0	$C_{15}H_{24}N_2O_2$
279	14.0	$C_{16}H_{27}N_2O_2$
293	13.0	$C_{17}H_{29}N_2O_2$
305	24.0	$C_{18}H_{29}N_2O_2$
321	14.0	$C_{18}H_{29}N_2O_3$
345	21.0	$C_{20}H_{29}N_2O_3$
409	20.0	$C_{25}H_{32}N_2O_3$
444	15.0	$C_{28}H_{32}N_2O_3$

Table (2-b): Mass spectrum for complex (4)

m/z	***Rel. Int.***	***Assignments***
55	30.0	C_4H_7
77	25.0	C_6H_{17}
91	21.0	C_6H_{19}
121	28.0	$C_7H_{21}O$
152	24.0	$C_8H_{24}O_2$
156	22.0	$C_8H_{28}O_2$
181	29.0	$C_{10}H_{29}O_2$
182	37.0	$C_{10}H_{30}O_2$
210	100.0	$C_{11}H_{32}NO_2$
224	32.0	$C_{12}H_3NO_2$
250	23.0	$C_{14}H_{36}NO_2$
288	26.0	$C_{16}H_{36}N_2O_2$
313	40.0	$C_{18}H_{37}N_2O_2$
349	21.0	$C_{21}H_{37}N_2O_2$
537	20.0	$C_{30}H_{37}N_2O_7$
552	15.0	$C_{31}H_{40}N_2O_7$
566	15.0	$C_{32}H_{42}N_2O_7$
663	16.0	$C_{32}H_{42}N_2O_9Zn$

Table (2-c): Mass spectrum for complex (17)

m/z	***Rel. Int.***	***Assignments***

55	47.0	C_4H_7
57	51.0	C_4H_9
71	29.0	C_5H_{11}
91	22.0	C_6H_{19}
120	25.0	C_8H_{23}
146	24.0	$C_{10}H_{26}$
182	17.0	$C_{13}H_{26}$
210	69.0	$C_{14}H_{26}O$
237	26.0	$C_{15}H_{27}NO$
239	39.0	$C_{15}H_{29}NO$
256	27.0	$C_{15}H_{30}NO_2$
281	44.0	$C_{17}H_{31}NO_2$
313	100.0	$C_{17}H_{31}NO_4$
339	28.0	$C_{19}H_{33}NO_4$
354	33.0	$C_{20}H_{36}NO_4$
368	73.0	$C_{20}H_{36}N_2O_4$
396	16.0	$C_{21}H_{36}N_2O_5$
452	15.0	$C_{23}H_{36}N_2O_7$
465	19.0	$C_{24}H_{37}N_2O_7$
479	15.0	$C_{25}H_{39}N_2O_7$
524	15.0	$C_{26}H_{40}N_2O_9$
552	21.0	$C_{27}H_{40}N_2O_{10}$
564	17.0	$C_{28}H_{40}N_2O_{10}$
576	16.0	$C_{29}H_{40}N_2O_{10}$
639	15.0	$C_{29}H_{40}CuN_2O_{10}$

3.3. IR spectra

IR spectral of the ligand and its metal complexes are showed in table **(3)** for the ligand, a centered band was appeared at 3423 cm^{-1} was due to υ(OH). In addition, strong bands appeared in 2926-2750 cm^{-1} and 2856-2480 cm^{-1} range indicating the presence of two types of intra- and intermolecular hydrogen bonds [26]. The higher frequency band was associated with a weaker hydrogen bond and the lower frequency corresponded to stronger hydrogen bond. The medium band appeared at 3300 cm^{-1} , was due to υ(NH), The spectrum showed bands at 1713 and 1607 cm^{-1} , corresponded to υ(C=O) and υ(C=N) respectively, and the bands observed at 1510,847 and 746 cm^{-1} , were due to vibrational of ν(Ar) ring. In order to know the mode of coordination of the ligand and its metal complexes. The IR spectra of the metal complexes were

compared with the ligand. The spectra of metal complexes showed bands in the 3570-3100 cm^{-1} range, corresponded to the presence of hydrated or coordinated water molecules. In addition, the bands appeared in 3650 - 2610cm^{-1} range were due to intra-and intermolecular hydrogen bonds [27]. The υ (NH) group appeared in the 3320 -3123 cm^{-1} range, however, the υ(C=O) and υ(C=N) bands were showed at 1719-1706 and 1630-1603 cm^{-1} ranges respectively [28]. The υ(NH) and υ(C=N) bands in spectra of metal complexes were shifted to lower frequency (lower region) indicating, coordination of NH amide and azomethine groups in the metal complexes. In acetate complexes, The acetate ion may be coordinated to the metal ion in unidentate manner [29]. As in the case of acetate complexes **(2)-(6)** bands appeared in the 1440-1434 and 1325-1286 cm^{-1} ranges were assigned to the asymmetric and symmetric stretches of the COO^- group. The mode of coordination of acetate group had been deduced from the magnitude of the observed separation between the υ_{asym} (COO^-) and υ_{sym} (COO^-), the separation value (Δ) between υ_{asym} (COO^-) and υ_{sym} (COO^-) in these complexes were 165-111 cm^{-1} range, suggesting that, the coordination of acetate group was in unidentate fashion [30]. The sulphate complexes **(7)-(12)** showed bands at 1272-1255, 1137-115, 1018-1013 and 762-745 cm^{-1} range, which assigned to monodentate sulphate group [31] .The chloro complexes **(13)-(16)**, and **(18)** showed band at 414-435 cm^{-1} range. Fe (III), complex **(10)** and Cr (III), complex **(11)** showed υ(C-O) at 1285 and 1280 cm^{-1} respectively, indicating that, the COH group coordinated to metal ion in an ionic state [32]. Finally, the complexes showed new bands at 647-515 and 572-432 cm^{-1} ranges which were assigned to υ(M-O) and υ(M-N) respectively [33].

Table (3). IR bands of the ligand [H_3L], (1) and its metal complexes.

No.	υ(H-bond)	υ(H2O)	υ(OH)	υ(NH)	υ(C=O)	υ(C=N)	υ(Ar)	υ(OAc)	υ(SO_4)	υ(-O-)	υ(M-O)	υ(M-N)	υ(M-Cl)
H_2L	3751-3200 2926-2600	3400-3255 3390-3130	3423, 1326	3300	1713	1607	1510, 746	-	-	1036	-	-	-
(2)	3600-3110 3100-2650	3250-3250 3450-3350	3420, 1320	3220	1719	1606	1509, 767	1438, 1286	-	1031	585	529	-
(3)	3620-2310 3300-2730	3440-3295 3280-3120	3422, 1321	3250	1717	1603	1510, 749	1434, 1295	-	1026	619	572	-
(4)	3650-3310 3300-2700	3470-3220 3470-3100	3425, 1320	3201	1718	1605	1511, 766	1440, 1285	-	1028	647	563	-

(5)	3650-3150 2240-2700	3500-3250 3240-3120	3435, 1318	3190	1718	1605	1510, 764	1438, 1320	-	1018	545	471	-
(6)	3650-2900 3190-2670	3565-3150 3450-3120	3423, 1322	3320	1718	1605	1511, 768	1436, 1325	-	1020	619	544	-

(7)	3650-3320 3310-2720	3520-3290 3280-3090	3418, 1325	3210	1719	1605	1510, 766	-	1260,1115,1017, 760	1030	614	434	-
(8)	3600-3310 3300-2670	3460-3255 3230-3070	3407, 1321	3319	1715	1608	1509, 765	-	1255, 1118, 1015,750	1027	615	455	-
(9)	3550-3280 3270-2710	3460-3255 3230-3130	3405, 1320	3250	1706	1608	1516, 750	-	1268,1130,1018, 762	1020	612	464	-
(10)	3565-3090 3200-2750	3540-3375 3360-3145	-	3195	1710	1618	1509, 754	-	1272, 1135, 1013, 755	1024	621	506	-
(11)	3600-3270 3260-2710	3470-3250 3240-3120	-	3251	1710	1627	1466, 749	-	1265, 1132, 1013, 755	1041	602	432	-
(12)	3575-3250 2340-2670	3490-/3240 3230-3170	3419, 1322	3190	1709	1630, 1622	1534, 760	-	1253, 1137, 1016, 738	1036	580	466	-
(13)	3570-3275 3270-2800	3490-3240 3200-3080	3423, 1319	3190	1717	1605	1509, 763	-	-	1022	541	445	414
(14)	3570-3310 3300-2750	3520-3310 3300-3120	3417, 1320	3220	1719	1605	1510, 767	-	-	1021	616	572	416
(15)	3600-3220 3210-2750	3550-3250 3240-3100	3450, 1323	3200	1716	1606	1510, 696	-	-	1028	562	476	419
(16)	3560-3330 3320-2650	3450-3270 3260-3120	3438, 1320	3210	1710	1620	1510, 742	-	-	1033	523	470	435
(17)	3570-3200 3190-2700	3450-3270 3260-3100	3409, 1318	3220	1717	1605	1509, 763	-	-	1043	578	516	-
(18)	3600-3250 3240-2800	3340-3220 3210-3070	3425, 1320	3219	1711	1606	1484, 743	-	-	1034	613	526	422
(19)	3560-3210 3200-2800	3550-3330 3310-3180	3425, 1322	3123	1717	1606	1510, 725	-	-	1029	593	470	-

3.4. Electronic spectra and magnetic moments

The electronic absorption data of the ligand and its metal complexes in dimethylsulphoxide (DMSO) are given in Table (**4**). The electronic absorption spectrum of the ligand showed three bands located at 288, 300 and 315 nm respectively. The first one was assigned to $\pi\rightarrow\pi^*$ transition which was nearly unchanged on complexation. The second and third bands were assigned to $n\rightarrow\pi^*$ and charge transfer transitions [34]. The electronic absorption spectrum of Cu(II) complexes **(2), (7)** and **(13)** showed bands at 298; 310; 465; 582 and 613, 285; 295; 310; 465; 562 and 610, 280; 295; 313; 435; 535 and 610 nm respectively. The first bands were due to intra-ligand transitions however, the other bands were corresponded to $^2B_{1g}(d_{x2-y2})\rightarrow{}^2A_{1g}d_{z2}$ (ν_1) $^2B_{1g}(d_{x2-y2})\rightarrow{}^2B_{2g}(d_{xy})$ (ν_2) and $^2B_{1g}(d_{x2-y2})\rightarrow{}^2E_g(d_{zy,}d_{xz})$ (ν_3) transitions [35]. The position as well as the broadness of these bands suggested that these complexes had distorted octahedral geometry around Cu (II) ions [36]. This could be due to the Jahn teller effect that operates on the d^9, electronic ground state of six coordinate system [36], elongating one *trans* pair of coordinate bonds and shortening the remaining four ones [37]. Magnetic moment values were found in the 1.69-1.71 B.M. range corresponding to one unpaired electron, spin-only value. The electronic absorption spectra of Mn(II) complex (**3**) showed bands at 280, 295, 312, 452, 562 and 630 nm. The first bands were corresponded to intra-ligand transitions however, the other bands indicating octahedral Mn(II) complex [38]. Zn(II) complex (**4**) showed bands at 282, 295 and 313 nm and Pb(II) complex **(6)** gave bands at 286, 297 and 311 nm and Mg(II) complex **(2)** gave 286, 298 and 311 nm and Bi(III) complex **(18)** gave 285, 298 and 313 nm and Sr(II) complex **(19)** showed bands at 285, 296 and 312 nm, corresponding to intra-ligand transitions these complexes showed diamagnetic property [39]. Ni(II) complexes **(5)** and **(8)** showed bands at 289, 292, 310, 425, 492, 582 and 735 and 286, 298, 312, 457, 583 and 742 nm respectively. The first bands were corresponded to intra-ligand transitions, however, the other bands were assigned to $^3A_{2g}(F)\rightarrow{}^3T_{2g}(F)(\nu_1)$, $^3A_{2g}(F)\rightarrow{}^3T_{1g}(\nu_2)$ and $^3A_{2g}(F)\rightarrow{}^3T_{1g}(P)(\nu_3)$ transitions respectively, which were consistent with octahedral geometry [40,41]. This observation is further confirmed by μ_{eff} values 3.25 and 3.02 B.M. corresponding to two unpaired electrons [42,43]. The ν_2/ν_1 ratio was 1.18 and 1.23 which were less than the usual range of octahedral Ni(II) complexes (1.5-1.7), indicating that, the Ni(II) complexes had distorted octahedral geometry [44]. Co(II) complexes **(9)** and **(14)** showed bands at 286, 290, 312,

465, 573 and 610 and 286, 296, 310, 460, 575 and 608 nm respectively. The first bands were due to intra-ligand transitions and the other bands indicating Co(II) octahedral structure which confirmed by M_{eff} = 4.38B.M. However, Fe(III) complex **(10)** gave bands at 285, 295, 308, 452, 571 and 620 nm. The first bands corresponding to intra-ligand transitions and the other bands indicating Fe(III) octahedral structure which confirmed by M_{eff} = 6.23 B.M. Cr(III), complex (**11**) showed bands at 285, 296, 310, 452, 535 and 612 nm. The first bands corresponding to intra-ligand transitions and the other bands confirmed octahedral Cr(III) complex, which confirmed by M_{eff}= 3.45 B.M [45], (Table 4)

Table (4):- Electronic spectra and magnetic moments for ligand and its some metal complexes

No. Of Compound	λ_{max} (nm)	$\mu_{eff.}$
(1)	288, 300, 315	-
(2)	298, 310, 465, 582, 613	1.70
(3)	280, 295, 312, 452, 562, 630	6.12
(4)	282, 295, 313	Diamagnetic
(5)	289, 292, 310, 425, 492, 582, 735	3.25
(6)	286, 297, 311	Diamagnetic
(7)	285, 295, 310, 465, 562, 610	1.71
(8)	286, 298, 312, 457, 583, 742	3.02
(9)	286, 290, 312, 465, 573, 610	4.37
(10)	285, 295, 308, 452, 571, 620	6.23
(11)	285, 296, 310, 452, 535, 612	3.45
(12)	286, 298, 313	Diamagnetic
(13)	280, 295, 313, 435, 535, 610	1.69
(14)	286, 296, 310, 460, 575, 608	4.38
(18)	2.85. 298, 313	Diamagnetic
(19)	285, 296, 312	Diamagnetic

3.5. Thermal analysis (DTA and TGA)

The Thermal data of complexes **(4)**, **(8)**, **(14)** and **(17)** shown in Table (5). These complexes were introduced as representative examples. The thermogram of complex **(4)** $[H_2L\ Zn(OAc)_2.H_2O].H_2O$ showed decomposition in several steps. The first step involving breaking of H-bondings accompanied by endothermic peak observed at 50^oC. In the second step, one molecule of hydrated water was lost endothermically with a peak at 80^oC accompanied by 2.80 % (Calc. 2.70 %) weight Loss. Loss of one coordinated water molecule was recorded in the third step as an endothermic peak appeared at 140^oC with

2.79 % (Calc. 2.72 %) weight loss. The 16.71 % weight loss (Calc. 17.80 %) accompanied by an endothermic peak observed at 280^{o}C, was assigned to loss of coordinated 2(OAc) group. Whereas the endothermic peak observed at 325^{o}C referred to the melting point of the complex. Loss of C_6H_5, $C_7H_6N_2$, and C_6H_4 groups with endothermic peaks observed at 330-365^{o}C range, with weight loss 42.02 % (Calc. 40.84 %). The final step observed as exothermic peaks observed at 400°C, 450°C, 560°C and 610°C with 28.05 % weight loss (Calc. 29.01%) referred to complete decomposition of the complex with exposed up with the formation of ZnO [46]. The Thermogram of complex **(8)** $[H_2L\ NiSO_4.2H_2O].5H_2O$ showed decomposition in several steps, The first step involving breaking of H-bondings accompanied with endothermic peak observed at 55^{o}C. In The second step, five molecules of hydrated water were lost endothermically with a peak at 95^{o}C accompanied by 2.61 % (Calc. 2.84 %) weight loss. Loss of two-coordinated water molecules were recorded in the third step as an endothermic peak observed at 150^{o}C with 2.81 % (Calc. 2.63 %) weight loss. The 13.25 % weight loss (Calc. 14.01 %) accompanied by an endothermic peak observed at 280^{o}C, was assigned to loss of coordinated SO_4 group. Whereas, the endothermic peak observed at 366^{o}C referred to the melting point of the complex. Loss of C_6H_5, $C_7H_6N_2$, and C_6H_4 groups with endothermic peaks observed at 375-490^{o}C range, with weight loss 36.06 % (Calc. 37.38 %). The final step observed as exothermic peaks observed at 580°C, 600°C, 630°C and 660°C with 35.93 % weight loss (Calc. 36.56 %) referred to complete decomposition of the complex with exposed up with the formation of NiO [47].The thermogram of complex**(14)** $[H_2LCoCl_2.H_2O].2H_2O$ showed decomposition in several steps. The first step involving breaking of H-bondings accompanied with endothermic peak observed at 55^{o}C. In the second step, two molecules of hydrated water were lost endothermically with a peak appeared at 85^{o}C accompanied by 2.91 % (Calc. 2.87 %) weight loss. Loss of one coordinated water molecule was recorded in the third step as an endothermic peak appeared at 135^{o}C with 2.90 % (Calc. 2.85 %) weight loss. The 15.59 % weight loss (Calc. 11.31 %) accompanied by an endothermic peak observed at 285^{o}C, was assigned to loss of 2(Cl) atoms. Whereas the endothermic peak observed at 335^{o}C referred to the melting point of the complex. Loss of C_6H_5, $C_7H_6N_2$, and C_6H_4 groups with endothermic peaks observed at 370-410^{o}C range, with weight loss 42.01 % (Calc. 43.15 %). The final step observed as exothermic peaks observed at 550^{o}C-630^{o}C range with 28.30 % weight loss (Calc. 29.97 %) referred to complete decomposition of the

complex with exposed up with the formation of CoO [48]. The thermogram of complex **(17)** $[H_2LCuCO_3.2H_2O].2H_2O$ showed decomposition in several steps. The first step involving breaking of H-bondings accompanied with endothermic peak at 50°C. In the second step, one molecule of hydrated water was lost endothermically with a peak appeared at 80°C accompanied by 2.42 % (Calc. 2.82 %) weight loss. Loss of two coordinated water molecules were recorded in the third step as an endothermic peak observed at 110°C with 2.41 % (Calc.2.80%) weight loss. The 10.01 % weight loss (Calc. 9.38 %) accompanied by an endothermic peak observed at 250°C, was assigned to loss of coordinated CO_3 group. Whereas the endothermic peak observed at 375°C referred to the melting point of the complex. Loss of C_6H_5, $C_7H_6N_2$, and C_6H_4 groups with endothermic peaks observed at 430-570°C range, with weight loss 40.98 % (Calc. 42.36 %). The final step observed as exothermic peaks observed at 590°C, 620°C, 650°C and 680°C with 35.97 % weight loss (Calc. 34.38 %) referred to complete decomposition of the complex with exposed up with the formation of CuO [49].

Table (5):- Thermal analyses for some metal (II) complexes

Compound No.	Temp. (°C)	DTA (peak)		TGA (Wt.loss %)		Assignments
		Endo	Exo	Calc.	Found	
Complex (4)	50	Endo	-	-	-	Broken of H-bondings
	80	Endo	-	2.70	2.80	Loss of (H_2O) hydrated water molecule
	140	Endo	-	2.72	2.79	Loss of (H_2O) coordinated water molecule
	280	Endo	-	17.78	16.71	Loss of 2(OAc) group
	325	Endo	-	-	-	Melting point
	330-365	Endo	-	40.84	42.02	Loss of (C_6H_5, $C_7H_6N_2$, C_6H_4)
	400-610	-	Exo	29.01	28.05	Decomposition process with the formation of ZnO (Residue)
Complex (8)	55	Endo	-	-	-	Broken of H-bondings
	95	Endo	-	2.84	2.61	Loss of 5(H_2O) hydrated water molecules
	150	Endo	-	2.63	2.81	Loss of 2(H_2O) coordinated water molecule
	280	Endo	-	14.01	13.25	Loss of SO_4 group
	366	Endo	-	-	-	Melting point
	375-490	Endo	-	37.38	36.06	Loss of (C_6H_5, $C_7H_6N_2$, C_6H_4)
	580-660	-	Exo	36.56	35.93	Decomposition process with the formation of NiO (Residue)
Complex (14)	65	Endo	-	-	-	Broken of H-bondings
	100	Endo	-	2.87	2.91	Loss of 2(H_2O) hydrated water molecule
	135	Endo	-	2.85	2.90	Loss of (H_2O) coordinated water molecule
	285	Endo	-	11.31	15.59	Loss of 2(Cl)
	335	Endo	-	-	-	Melting point
	370-410	Endo	-	43.15	42.01	Loss of (C_6H_5, $C_7H_6N_2$, C_6H_4)
	550-630	-	Exo	29.97	28.30	Decomposition process with the formation of CoO (Residue)
Complex (17)	50	Endo	-	-	-	Broken of H-bondings
	80	Endo	-	2.82	2.42	Loss of 2(H_2O) hydrated water molecules
	110	Endo	-	2.80	2.41	Loss of 2(H_2O) coordinated water molecules

	250	**Endo**	**-**	**9.38**	**10.01**	**Loss of (CO_3) group**
	375	**Endo**	**-**	**-**	**-**	**Melting point**
	430-570	**Endo**	**-**	**42.36**	**40.98**	**Loss of (C_6H_5, $C_7H_6N_2$, C_6H_4)**
	590-680	**-**	**Exo**	**34.38**	**35.97**	**Decomposition process with the formation of CuO (Residue)**

3.6. ^{1}H-NMR spectra of the ligand and its Zn (II), complex (4)

The ^{1}H-NMR spectrum of the ligand (H_2L) showed the absence of the signal of the amino group (NH_2) characteristic of the starting material (hydrazide). The spectrum showed three sets of peaks, the first one observed as singlet at 11.60 (w, 1H), 8.20 (s, 1H) and 4.35 (s, 1H) ppm which may be assigned aromatic hydroxyl proton, azomethine proton and NH proton respectively [50]. The second set appeared as multiplets in the 6.82-7.92 ppm range, which were attributed to aromatic protons. The group appeared at 2.50-3.50 (s, 3H), (s, 2H) ppm range referred to aliphatic groups CH_3 and CH_2 respectively [51]. Comparing the ^{1}H-NMR protons of azomethine was still present, a significant downfield shift of the azomethine proton signal in the complexes relative to the corresponding signal of the free ligand confirmed the coordination of the azomethine nitrogen atom to the metal. For the spectrum of the Zn(II) complex **(4)** with that of the free ligand, it was noticed that a significant downfield shift of the hydroxyl and azomethine proton signals in the complex relative to the corresponding signal of the free ligand confirmed the coordination of the hydroxyl oxygen and the azomethine nitrogen atoms to Zn(II) ion [52]. The signals due to the proton of the hydroxyl OH and azomethine group appeared at 10.40 and 7.98 ppm, however, the NH proton appeared at 4.2 ppm. The signals corresponding to aromatic protons appeared at 6.80-7.82 ppm range. The protons due to CH_3 and CH_2 appeared at 2.45-3.66 ppm range. The signal appeared at 1.43 ppm, may be due to the protons of acetate group [53].

Figure (1): ^{1}H-NMR spectra of the ligand

Figure (2): ^{1}H-NMR spectra of the ligand Zn (II), complex (4)

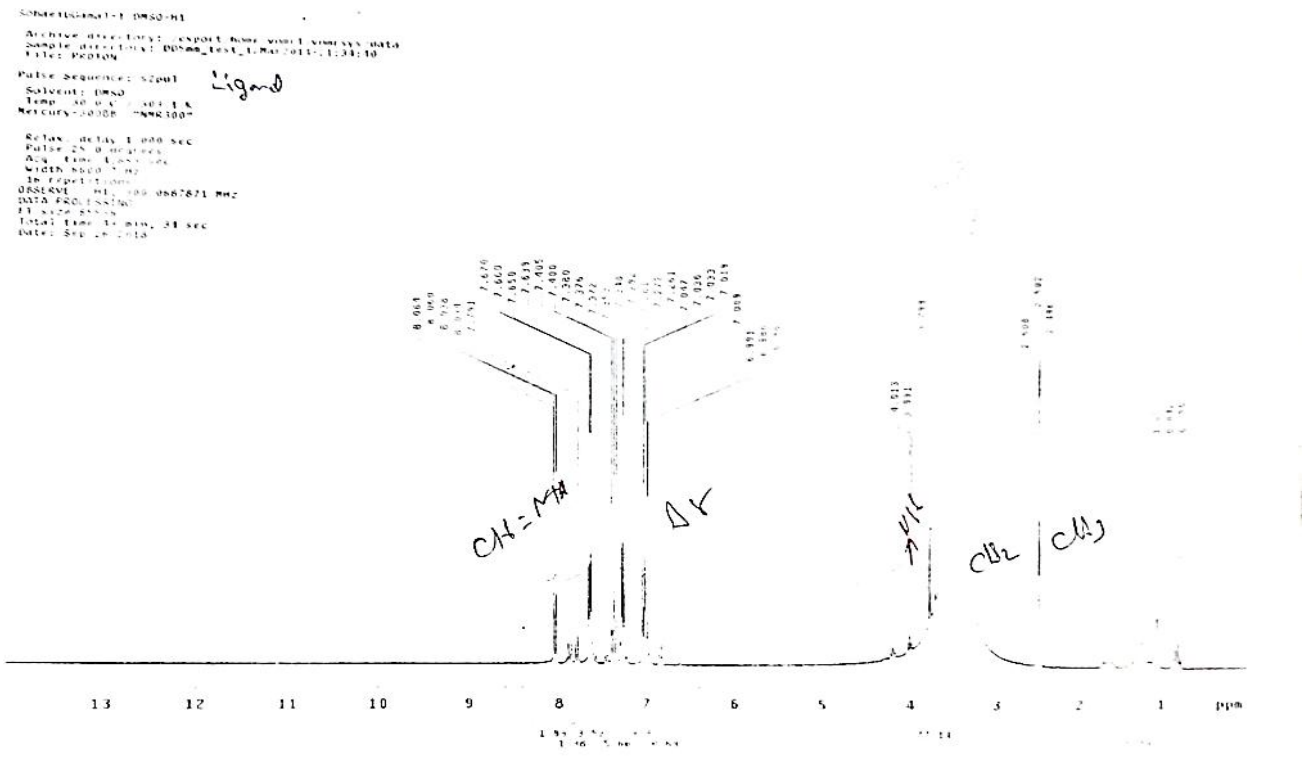

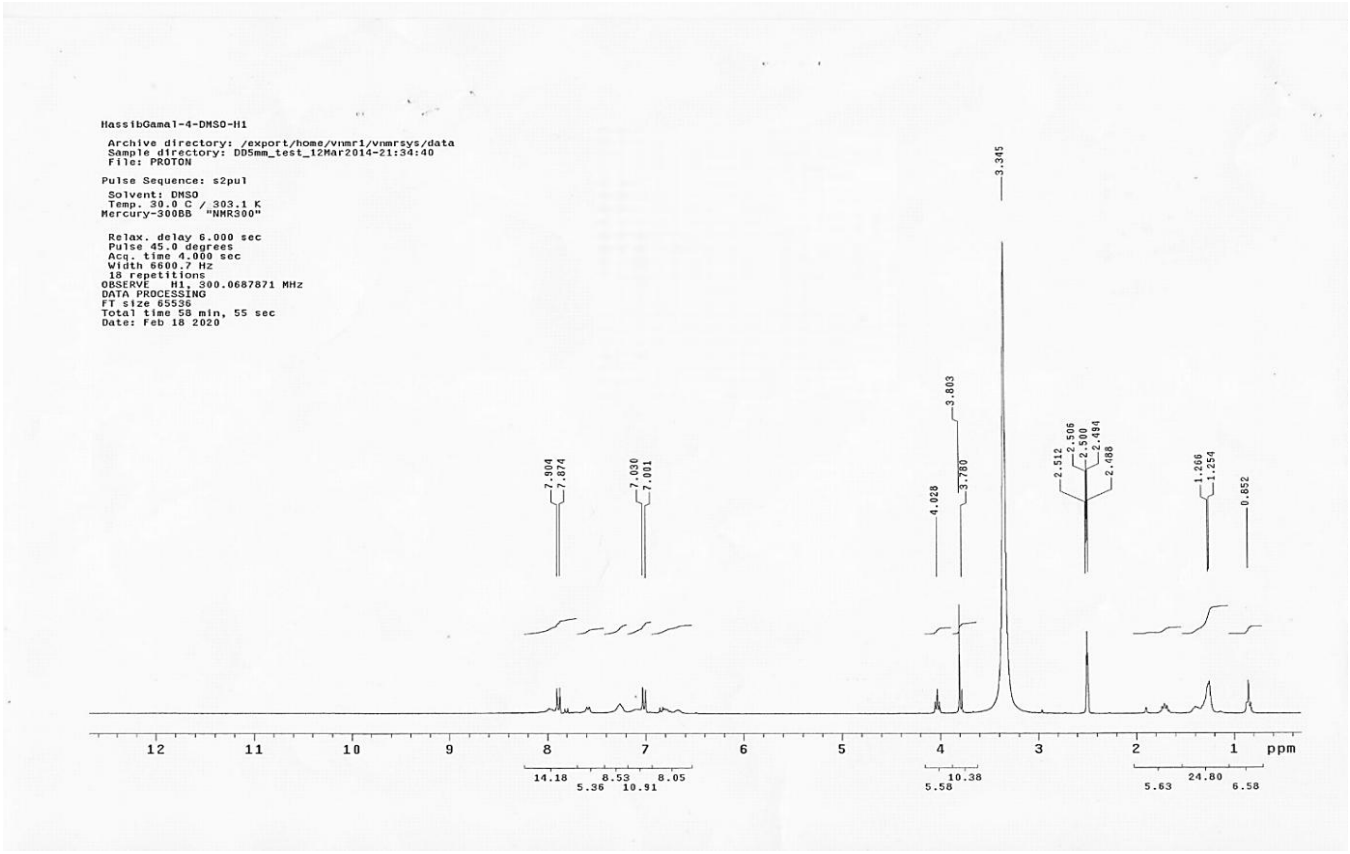

3.7. Electron spins resonance (ESR)

The ESR spectral data for complexes **(2), (3), (7), (9), (10), (11)** and **(13)** presented in table (**6**). The spectra of copper(II) complexes **(2), (7)** and **(13)** are characteristic of species, d^9configuration having axial type of a $d(x^2-y^2)$ ground state which is the most common for copper(II) complexes [54,55]. The complexes showed $g_{\|} > g_{\perp} > 2.0023$, indicating octahedral geometry around the copper(II) ion [56,57]. The g-values are related by the expression $G = (g_{\|}-2)/(g_{\perp}-2)$, where (G) is an exchange coupling interaction parameter. If $G < 4.0$, a significant exchange coupling is present, whereas if G value **≥** 4.0, local tetragonal axes are aligned parallel or only slightly misaligned. Complexes showed values < 4.0 (Table 6), indicating spin-exchange interactions took place between copper(II) ions. This phenomena is further confirmed by the magnetic moments values (Table 6). The $g_{\|}$ / $A_{\|}$ value is also considered as a diagnostic term for stereochemistry, the $g_{\|}/A_{\|}$ values were found in the 173.1-226 cm^{-1} range, indicating distorted octahedral copper(II) complexes [58]. The g-value of the copper(II) complexes with a $2B_{1g}$ ground state ($g_{\|}>g_{\perp}$) may be expressed by:[58]

$$\mathbf{g_{\|} = 2.002 - (8K^2_{\|}\,\lambda°/\Delta E_{xy})} \qquad \mathbf{(2)}$$

$$g_{\perp} = 2.002 - (2K^2_{\perp}\lambda^{\circ}/\Delta E_{xz}) \quad (3)$$

Where $k_{\parallel}$ and $k_{\perp}$ are the parallel and perpendicular components respectively of the orbital reduction factor (K), λ° is the spin-orbit coupling constant for the free copper, ΔE_{xy} and ΔE_{xz} are the electron transition energies of $2B_{1g} \rightarrow 2B_{2g}$ and $2B_{1g} \rightarrow 2E_g$. From the above relations, the orbital reduction factors ($K_{\parallel}$, $K_{\perp}$, K), which are measured terms for covalency [59], can be calculated. For an ionic environment, K=1; while for a covalent environment, K<1. The lower the value of K, the greater is the covalency. The above equations can be arranged as follow :-

$$K^2_{\perp} = (g_{\perp} - 2.002)\,\Delta E_{xz}\,/2\lambda_o \quad (4)$$

$$K^2_{\parallel} = (g_{\parallel} - 2.002)\,\Delta E_{xy}\,/8\lambda_o \quad (5)$$

$$K^2 = (K^2_{\parallel} + 2K^2_{\perp})/3 \quad (6)$$

K values for the copper(II) complexes **(2), (7)** and **(13)** indicated covalent bond character [60,61]. Kivelson and Neiman noted that, for ionic environment $g_{\parallel} \geq 2.3$ and for a covalent environment $g_{\parallel} < 2.3$. Theoretical work by Smith seems to confirm this view [62]. The g-values reported here, Table (6) showed considerable covalent bond character. Also, the in-plane σ-covalency parameter, α^2(Cu) was calculated by :-

$$\alpha^2(Cu) = (A_{\parallel}/0.036) + (g_{\parallel} - 2.002) + 3/7(g_{\perp} - 2.002) + 0.04 \quad (7)$$

The calculated values (Table 6) suggested a covalent bonding character. The in-plane and out of-plane π- bonding coefficients β_1^2 and β^2 respectively, are dependent upon the values of ΔE_{xy} and ΔE_{xz} as shown in the following equations [63].

$$\alpha^2\beta^2 = (g_{\perp} - 2.002)\,\Delta E_{xy}/2\lambda o \quad (8)$$

$$\alpha^2\,ß_1^2 = (g_{\parallel} - 2.002)\,\Delta E_{xz}/8\lambda o \quad (9)$$

In this work, the complexes **(2), (7)** and **(13)** showed β_1^2 values 1.09, 0.98 and 1.03 indicating moderate degree of covalency in the in-plane π-bonding [64,65]. However, the complexes showed β^2 indicating ionic bond character of the out-of-plane. It is possible to calculate approximate orbital populations for d orbitals by:

$$A_{\parallel} = A_{iso} - 2B[1 \pm (7/4)\,\Delta g_{\parallel}] \quad \Delta g_{\parallel} = g_{\parallel} - g_e \quad (10)$$

$$a^2_d = 2B/\,2B^{\circ} \quad (11)$$

Where A° and 2B° is the calculated dipolar coupling for unit occupancy of d orbital respectively. When the data are analyzed, the components of the Cu hyperfine coupling were considered with all the sign combinations [66]. The only physically meaningful results found when $A_{\parallel}$ and $A_{\perp}$ were negative. The resulting isotropic coupling constant was negative and the parallel component of the dipolar coupling 2B were negative (Table 6). These results can only occur for an orbital involving the $d_{(x2-y2)}$ atomic orbital on copper. The value for 2B is quite normal for copper(Il) complexes. The $|A_{iso}|$ value was relatively small. The 2B value divided by $2B_o$. The calculated dipolar coupling for unit occupancy of $d_{(x2-y2)}$. Using equation (11) suggested all orbital population were 52.8, 96.7, 52.7 % d-orbital spin density, clearly the orbital of the unpaired electron is $d_{(x2-y2)}$ [67]. However, Mn(II) complex (**2**), Co(II) complex (**9**), Fe(III) complex (**10**) and Cr(III) complex (**11**) showed isotropic spectra with g_{iso} 2.05, 2.03, 2.01 and 2.02 respectively confirming covalent bond character [68].

Table (6):- ESR spectral data of some metal complexes

Com pNo.	$g_{\parallel}$	$g_{\perp}$	g_{iso}[a]	$A_{\parallel}$ (G)	$A_{\perp}$ (G)	A_{iso}[o] (G)	G[c]	ΔE_{xy} (cm^{-1})	ΔE_{xz} (cm^{-1})	$K_{\perp}^2$	$K_{\parallel}^2$	K^2	K	$g_{\parallel}/A_{\parallel}$ (cm^{-1})	α^2	β^2	$^1\beta_2$	-2β	a^2d (%)
(2)	2.26	2.08	2.14	130	10	50	3.25	17182	21505	1.0	0.67	0.89	0.94	226	0.61	1.64	1.09	124	52.8
(3)	-	-	2.05	-	-	-	-	-	-	-	-	-	-	-	-	-	-	-	-
(7)	2.20	2.06	2.11	110	5	40	3.1	17793	21505	0.75	0.53	0.68	0.82	220	0.54	1.38	0.98	227	96.7
(9)	-	-	2.03	-	-	-	-	-	-	-	-	-	-	-	-	-	-	-	-
(10)	-	-	2.01	-	-	-	-	-	-	-	-	-	-	-	-	-	-	-	-
(11)	-	-	2.02	-	-	-	-	-	-	-	-	-	-	-	-	-	-	-	-

3.8. Chemical structures of the ligand and its metal complexes

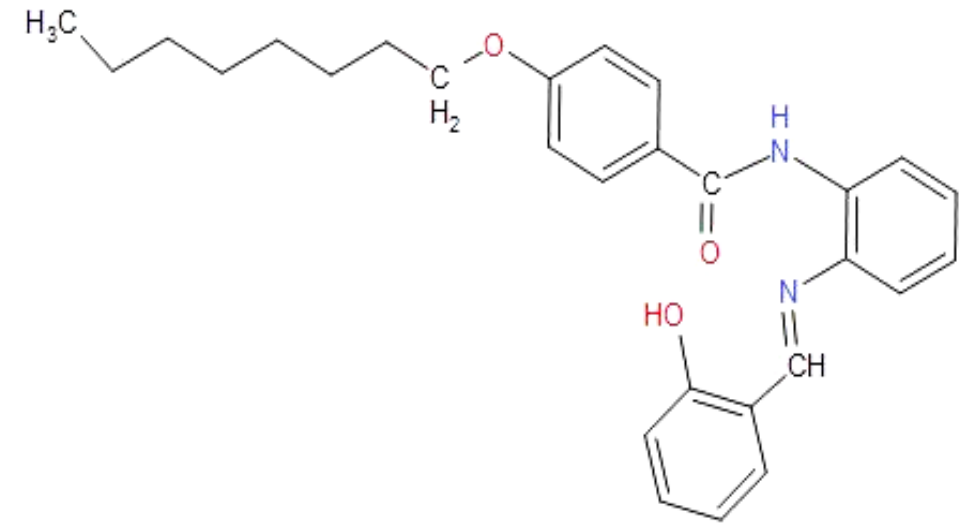

Ligand

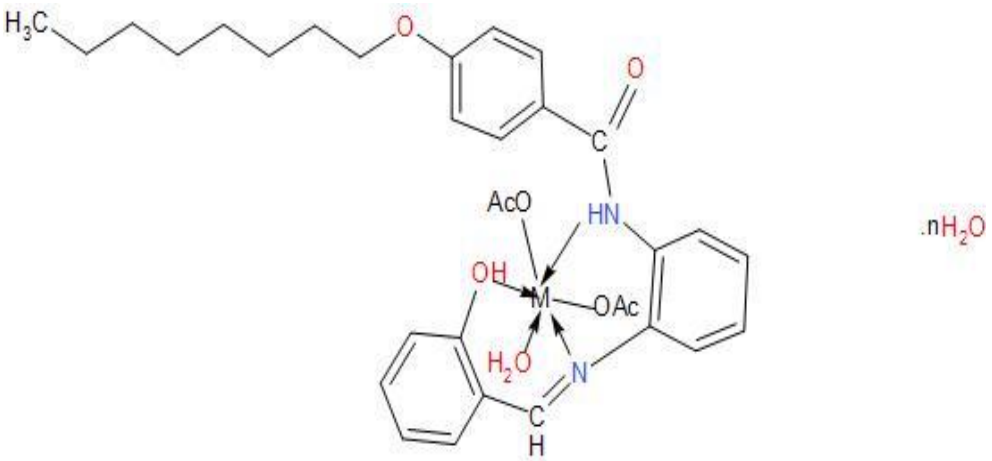

Complex **(2)** M = Cu(II), n = H_2O .
Complex **(3)** M = Mn(II), n = 3 H_2O .
Complex **(4)** M = Zn(II), n = H_2O .
Complex **(5)** M = Ni(II), n = H_2O .
Complex **(6)** M = Pb(II), n = H_2O .

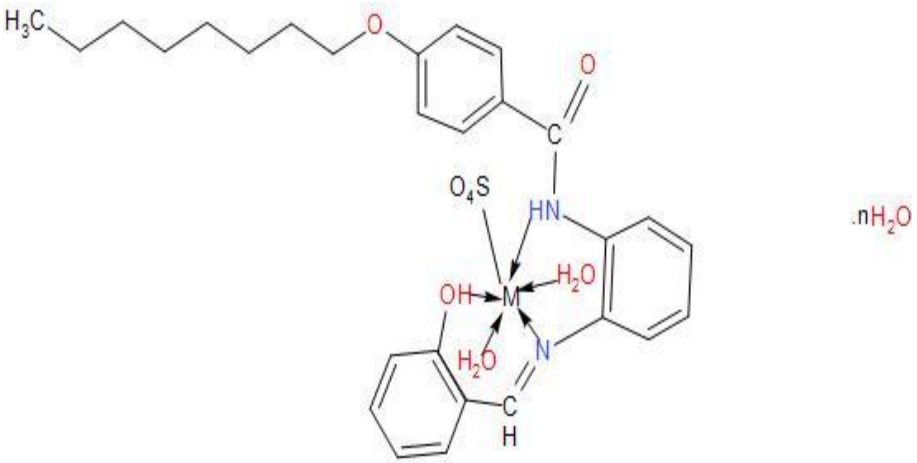

Complex **(7)** M = Cu(II), n = H_2O
Complex **(8)** M = Ni(II), n = 5 H_2O .
Complex **(9)** M = Co(II), n= 3 H_2O.
Complex **(12)** M = Mg(II), n = 5 H_2O.

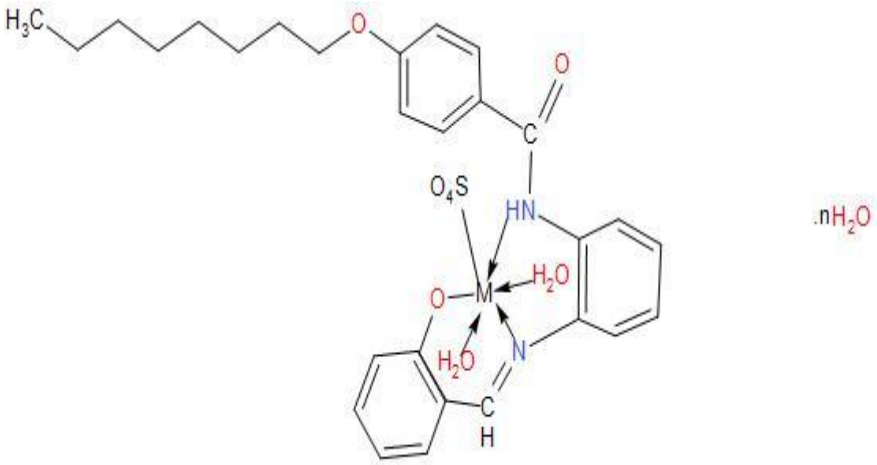

Complex **(10)** M = Fe(III). n= 2 H_2O
Complex **(11)** M = Cr(III). n= 2 H_2O

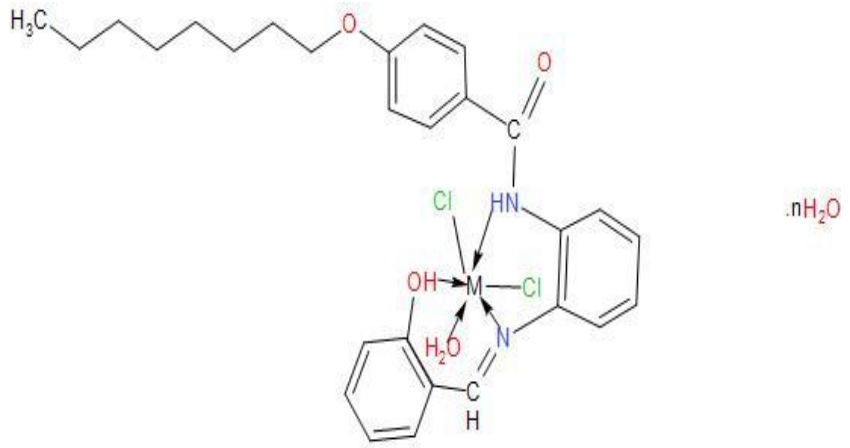

Complex **(13)** M = Cu(II), n = H_2O.
Complex **(14)** M = Co(II), n = 2 H_2O .
Complex **(15)** M = Ba(II), n = 3 H_2O .
Complex **(16)** M = Sr(II). n = H_2O

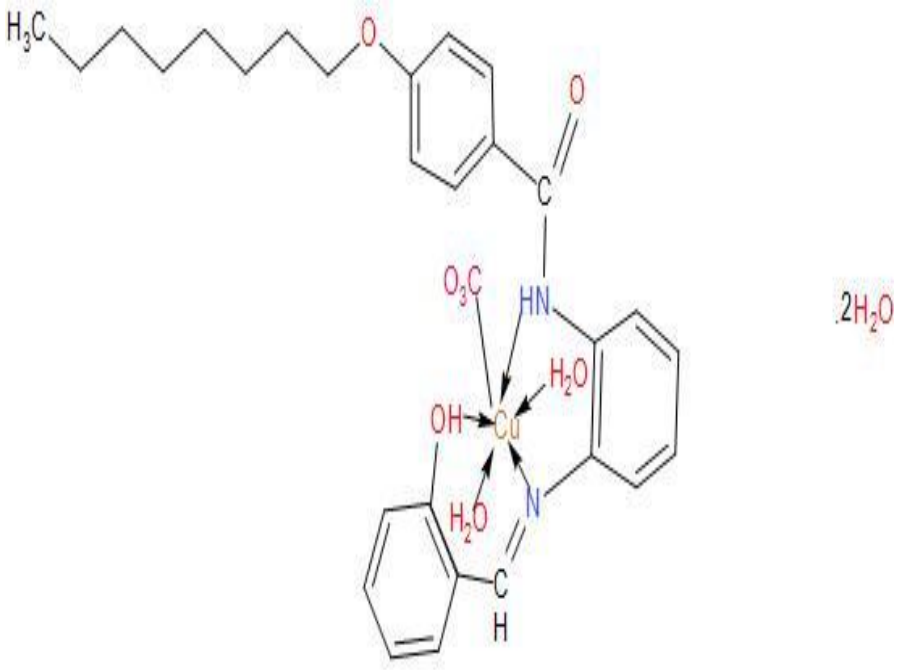

Complex **(17)**

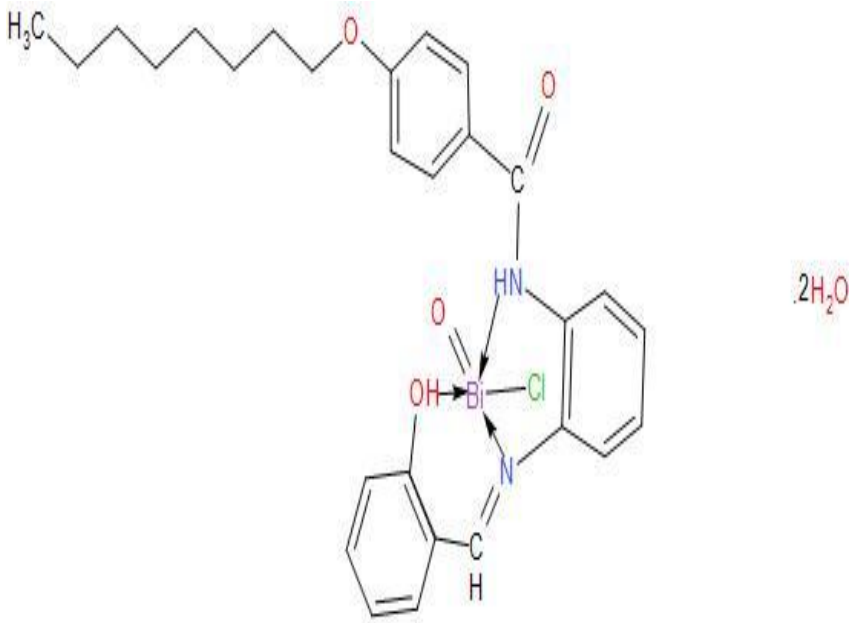

Complex **(18)**

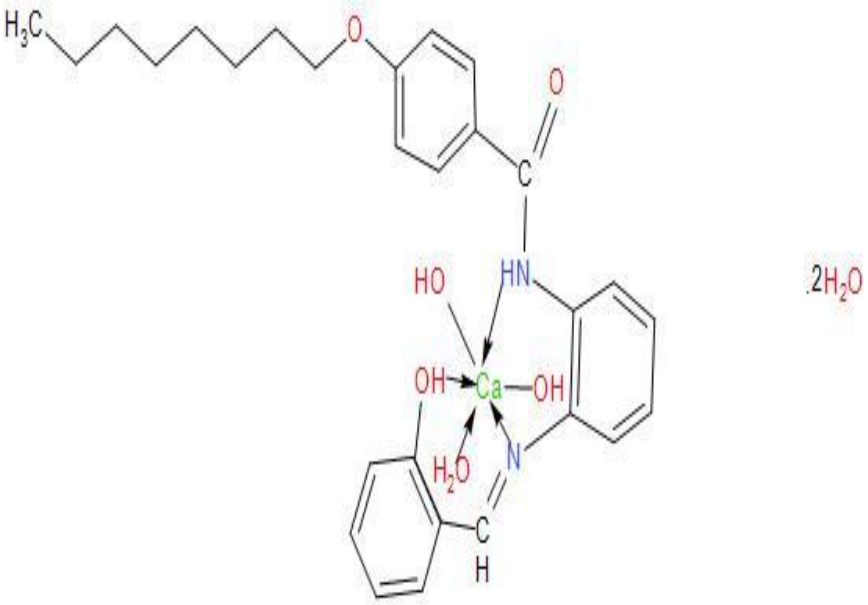

Complex **(19)**

Figure (3): Molecular structures of the formed ligand and its some metal complexes

3.9. Biological studies

3.9.1. Invitro Study, cytotoxicity Effect

The cytotoxic activity of some metal complexes **(2)**, **(3)**, **(4), (5) and (15)** was evaluated against human breast cancer cell line (MCF-7), the IC50 values were calculated for the complexes, and the results were presented in Figure **(4-32)**. As shown, most complexes displayed significantly cytotoxic activities compared to the standard drug (Cisplatin). Cytotoxicity activity of the complexes may attribute to the central metal atom, which was explained by Tweedy's chelation theory [69]. Copper (II) complex **(2)** showed the highest cytotoxicity effect with IC_{50} value of 6.31 μM, followed by nickel (II) complex **(5)** with IC_{50} value 12.3 μM, then zinc (II) complex **(4)** with IC_{50} value 13.4 μM, manganese (II) complex **(3)** with IC_{50} value 23.4 and eventually barium (II) complex **(15)** with IC_{50} value 29 μM. It was observed that an enhancement of the antitumor activity occurs by coordination [70]. The enhancement of cytotoxic activity may be assigned to that the positive charge of the metal increased the acidity of coordinated ligand that bears protons, leading to stronger hydrogen bonds which enhanced the biological activity [71]. It seems that, changing the anion, coordination sites, and the nature of the metal ion has a pronounced effect on the biological behavior by altering the binding ability of DNA [72]. Gaetke and Chow had reported that, metal has been suggested to facilitate oxidative tissue injury through a free radical mediated pathway analogous to the Fenton reaction [73]. By applying the ESR-trapping technique, evidence for metal - mediated hydroxyl radical formation in vivo has been obtained [74]. Reactive oxygen species are produced through a Fenton-type reaction as follows:

$$\mathbf{LM(II) + H2O2 \rightarrow LM(I) +.OOH + H+}$$

$$\mathbf{LM(I) + H_2O_2 \rightarrow LM(II) +.OH + OH^-}$$

Where L, organic ligand

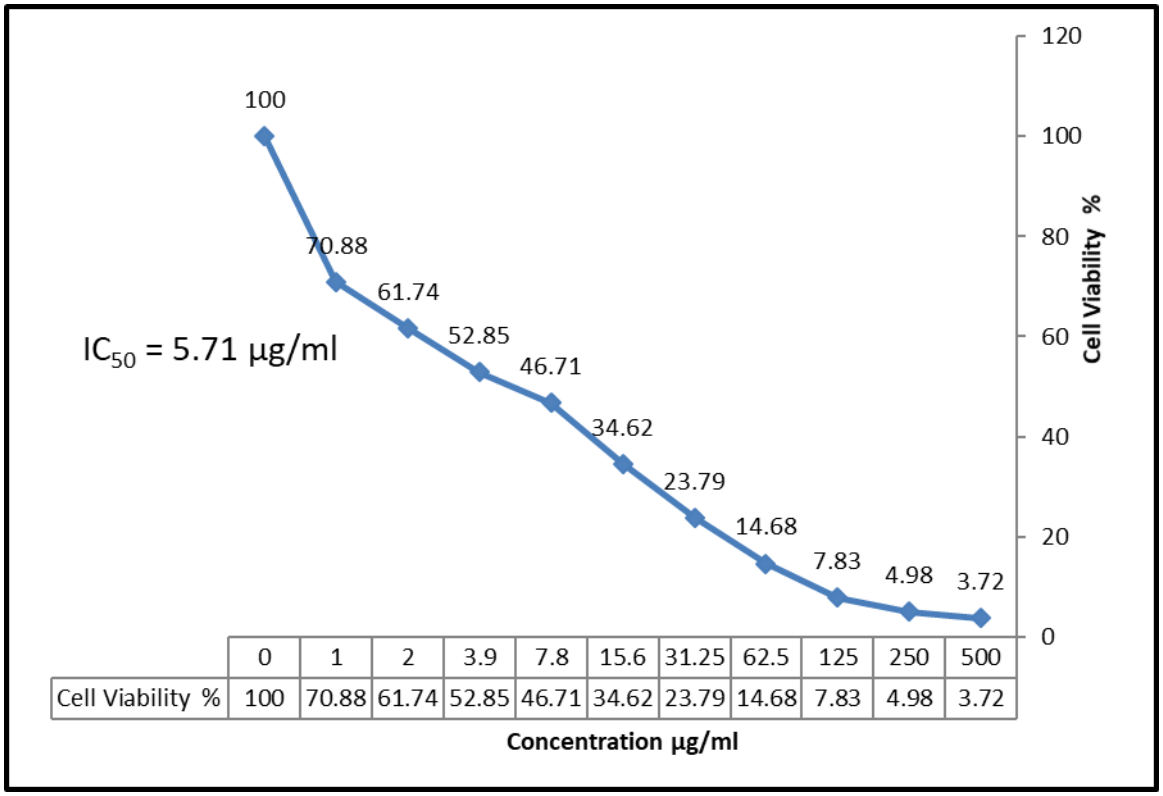

Figure (4): Histogram for cytotoxic activity and IC_{50} value of Standard drug (Cisplatin)

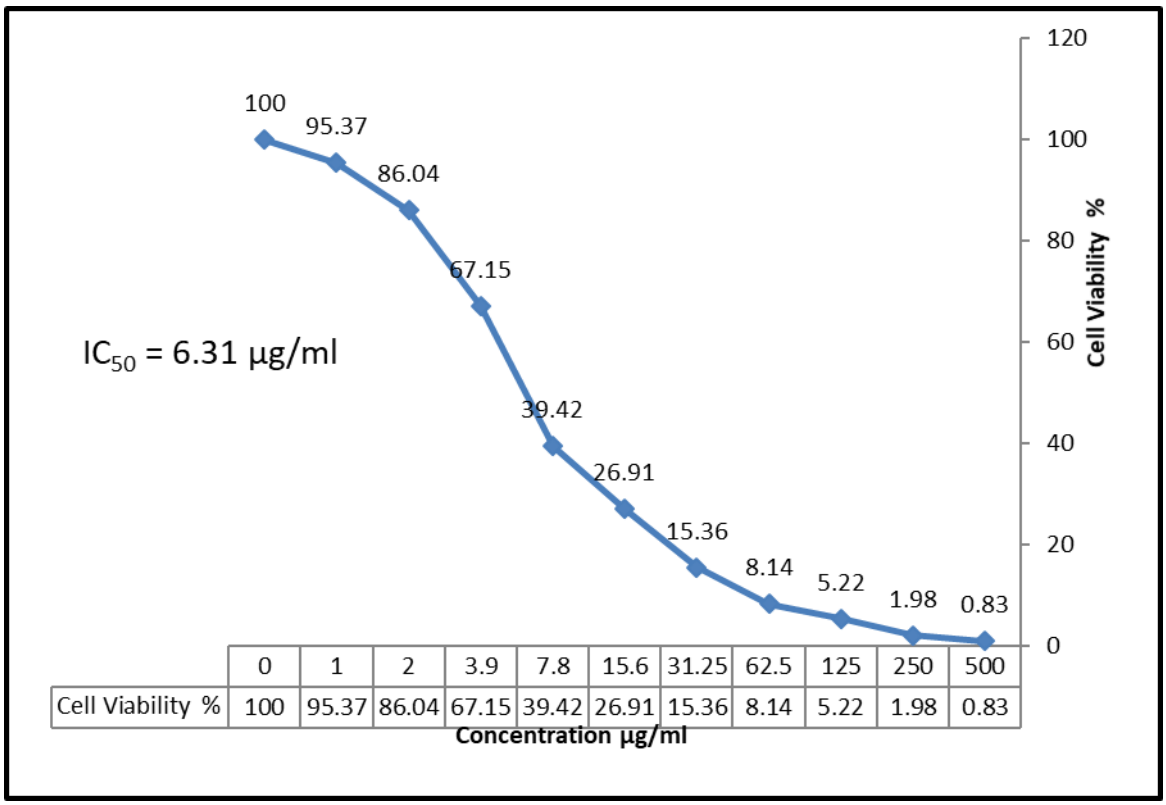

Figure (5): Histogram for cytotoxic activity and IC_{50} value of Cu (II) Complex (2)

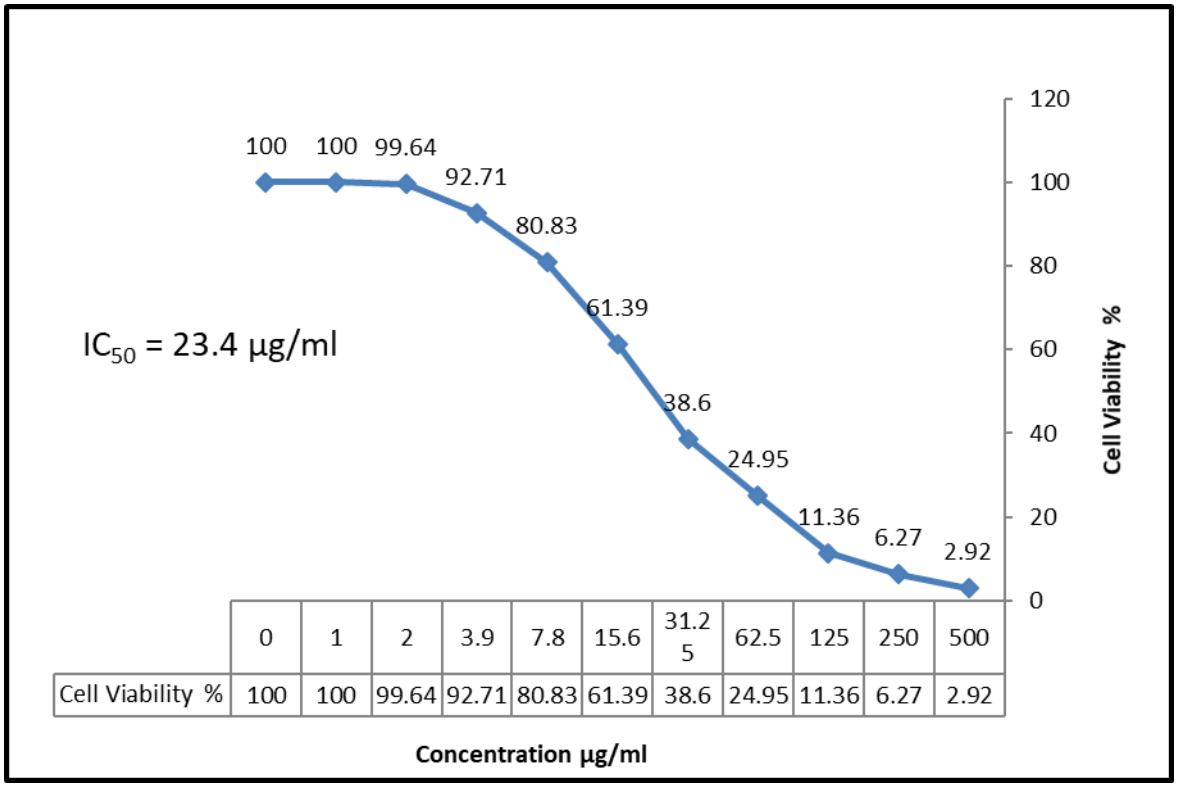

	0	1	2	3.9	7.8	15.6	31.25	62.5	125	250	500
Cell Viability %	100	100	99.64	92.71	80.83	61.39	38.6	24.95	11.36	6.27	2.92

Figure (6): Histogram for cytotoxic activity and IC50 value of Mn (II) Complex (3)

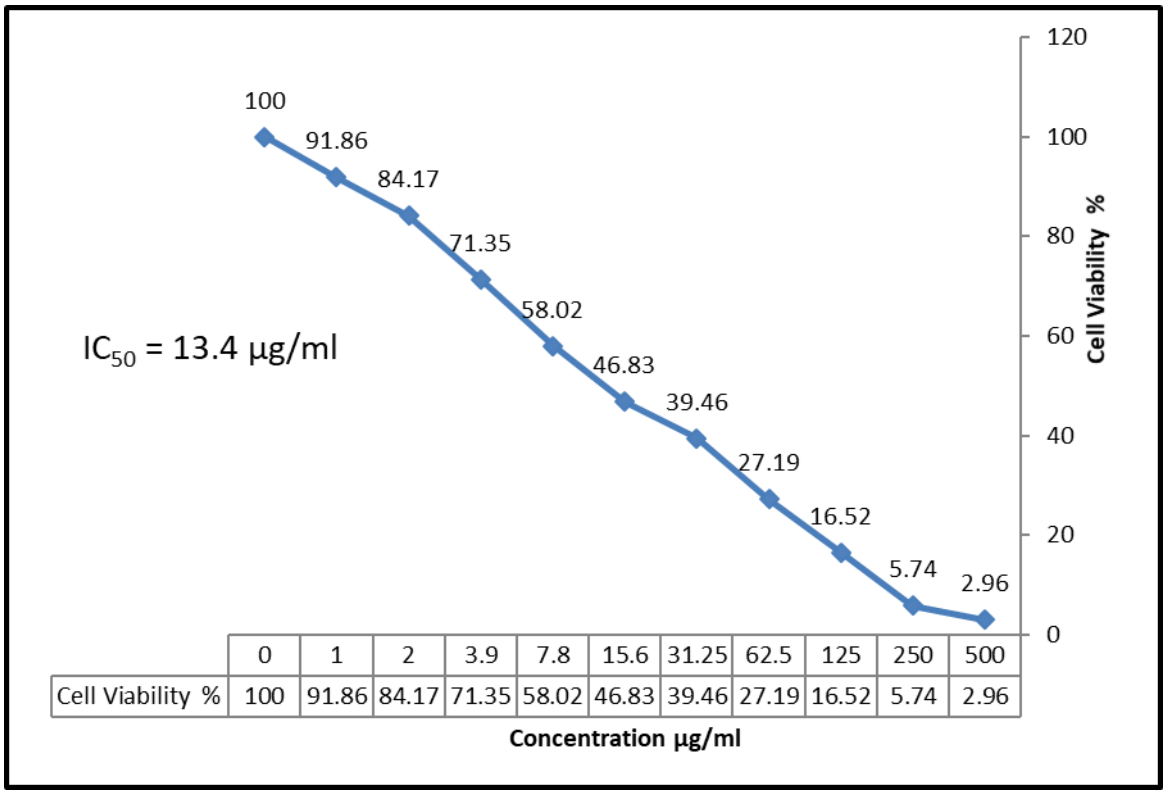

	0	1	2	3.9	7.8	15.6	31.25	62.5	125	250	500
Cell Viability %	100	91.86	84.17	71.35	58.02	46.83	39.46	27.19	16.52	5.74	2.96

Figure (7): Histogram for cytotoxic activity and IC50 value of Zn (II) Complex (4)

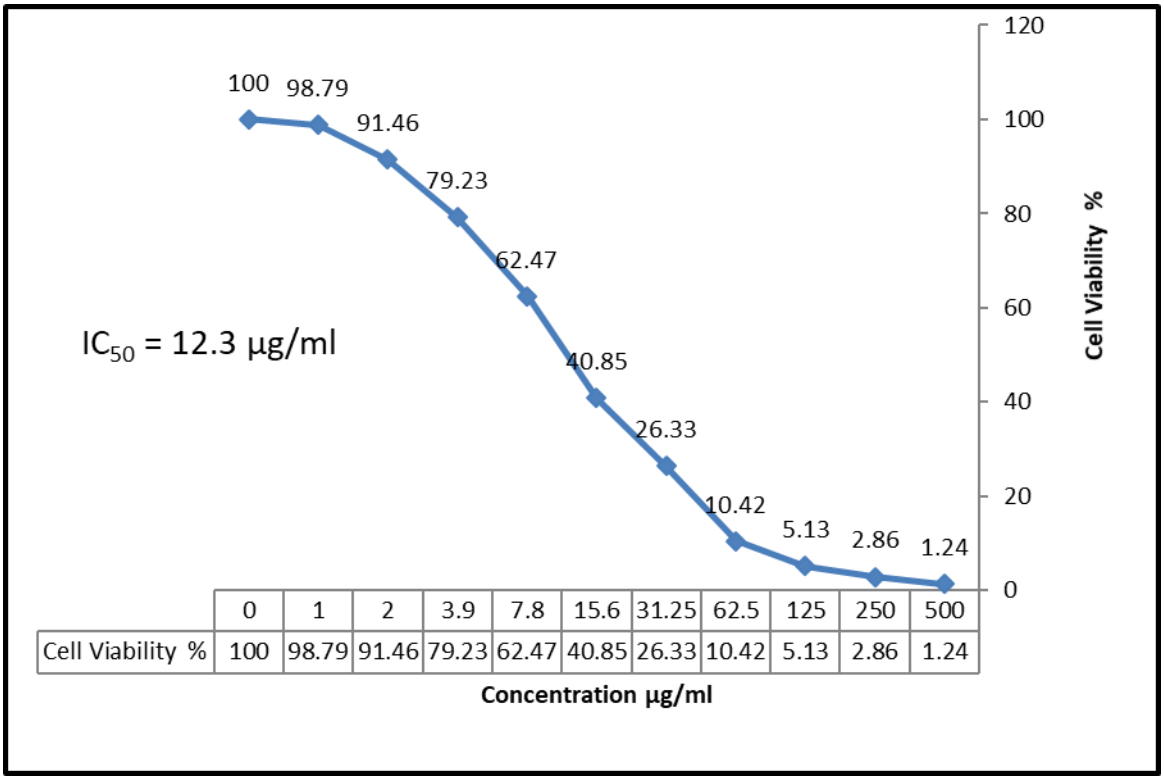

Figure (8): Histogram for cytotoxic activity and IC50 value of Ni (II) Complex (5)

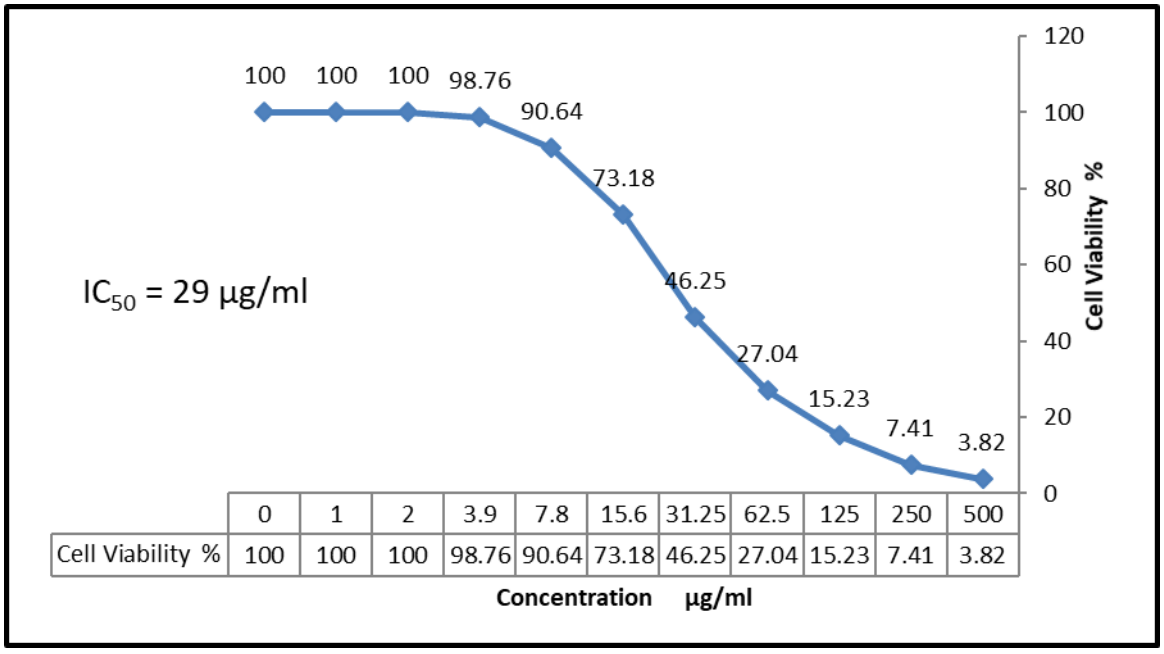

Figure (9): Histogram for cytotoxic activity and IC50 value of Ba (II) Complex (15)

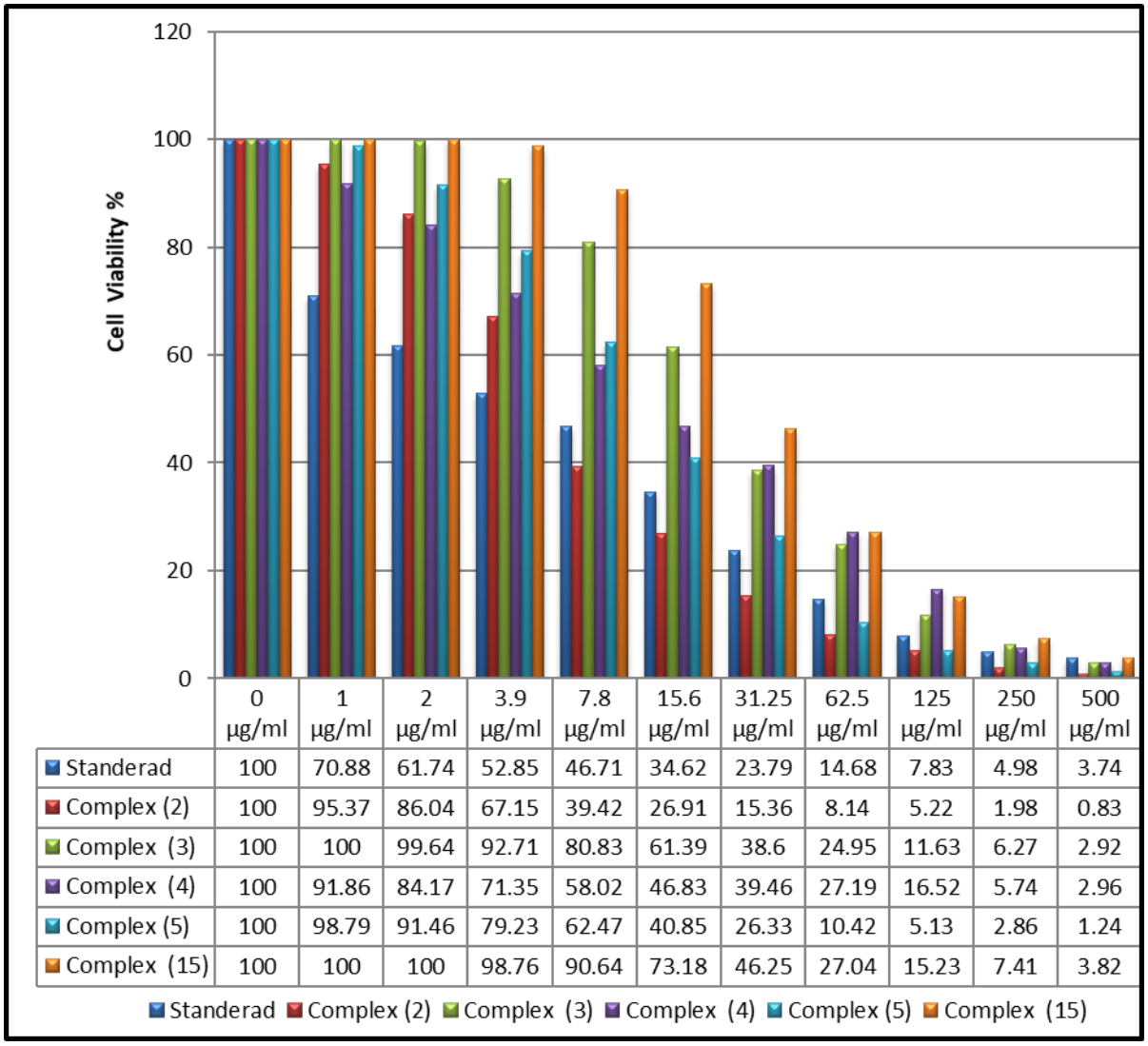

	0 µg/ml	1 µg/ml	2 µg/ml	3.9 µg/ml	7.8 µg/ml	15.6 µg/ml	31.25 µg/ml	62.5 µg/ml	125 µg/ml	250 µg/ml	500 µg/ml
Standerad	100	70.88	61.74	52.85	46.71	34.62	23.79	14.68	7.83	4.98	3.74
Complex (2)	100	95.37	86.04	67.15	39.42	26.91	15.36	8.14	5.22	1.98	0.83
Complex (3)	100	100	99.64	92.71	80.83	61.39	38.6	24.95	11.63	6.27	2.92
Complex (4)	100	91.86	84.17	71.35	58.02	46.83	39.46	27.19	16.52	5.74	2.96
Complex (5)	100	98.79	91.46	79.23	62.47	40.85	26.33	10.42	5.13	2.86	1.24
Complex (15)	100	100	100	98.76	90.64	73.18	46.25	27.04	15.23	7.41	3.82

Figure (10): Histogram for cytotoxic activity of complexes against MCF-7 cell line

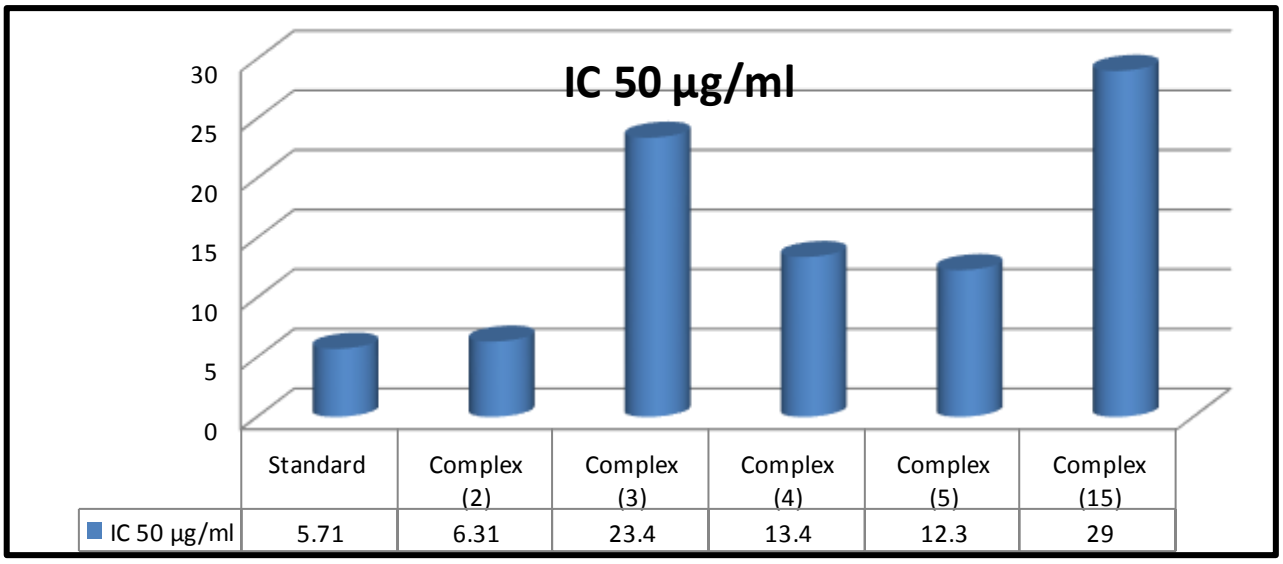

	Standard	Complex (2)	Complex (3)	Complex (4)	Complex (5)	Complex (15)
IC 50 µg/ml	5.71	6.31	23.4	13.4	12.3	29

Figure (11): Histogram of IC_{50} value for some of metal complexes

The microscopic images showed the chemotherapeutic activity of the tested complexes by comparing them with the standard drug (Cisplatin) as shown below. There is decreasing in the number of available cells. Most of the remaining observed degeneration changespresented in the form of irregulatory cell membrane, opaque and not well formed chromatin regulated of swalling cytoplasm, other showed optatic changes in the form of chrunked cells, increase in eosinophilia cells, and picknitoic nucleus as shown in figures 12-32

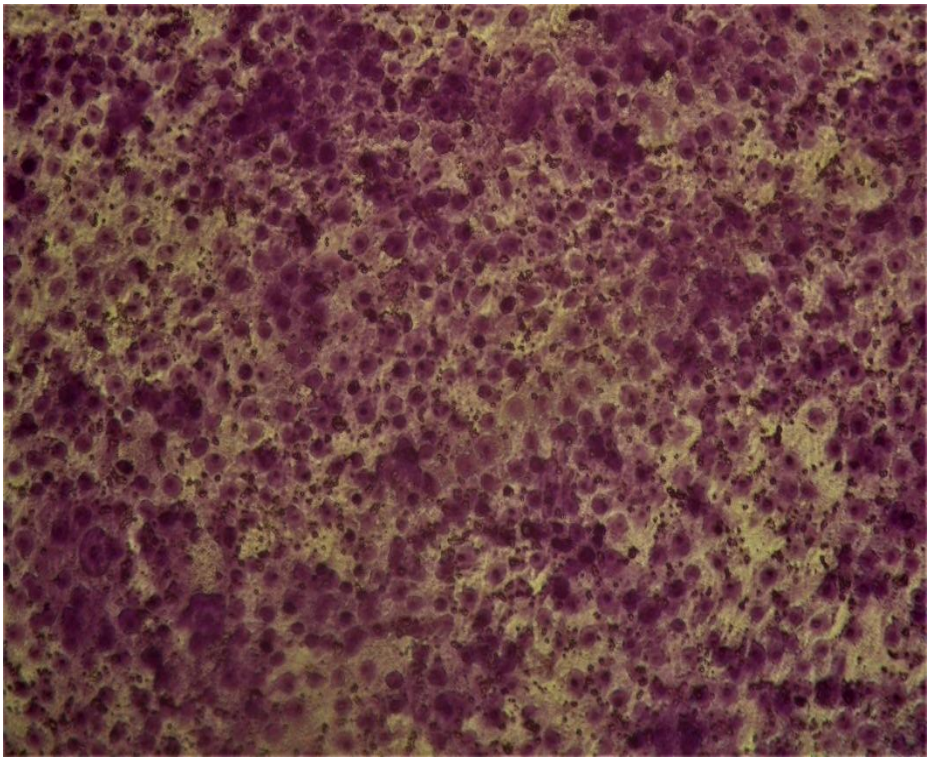

Figure (12): MCF-7 control Untreated

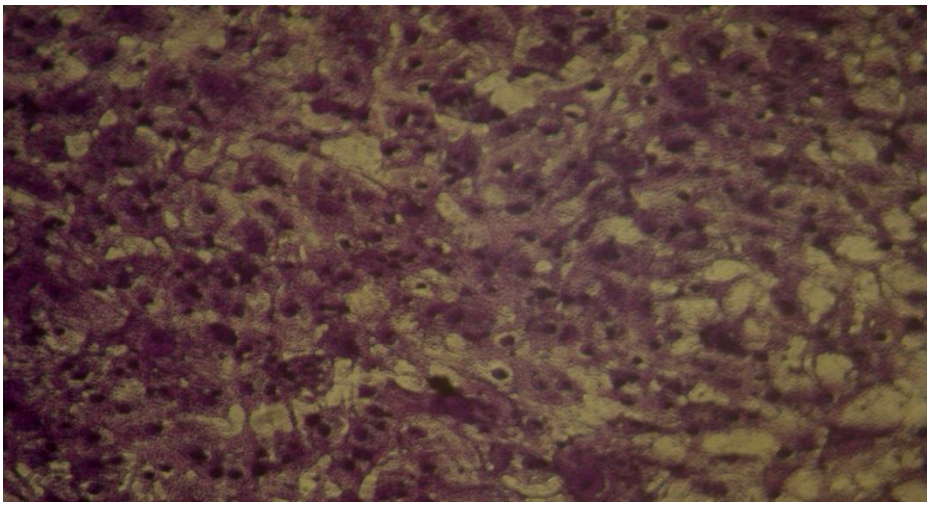

Figure (13): MCF-7 cells treated with Cu(II) complex (2) at 4µg

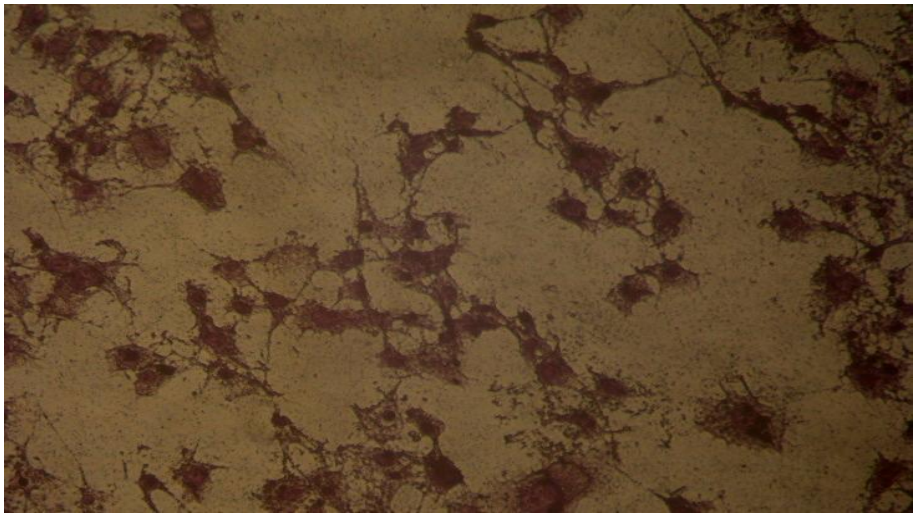

Figure (14): MCF-7 cells treated with Cu(II) complex (2) at 10µg

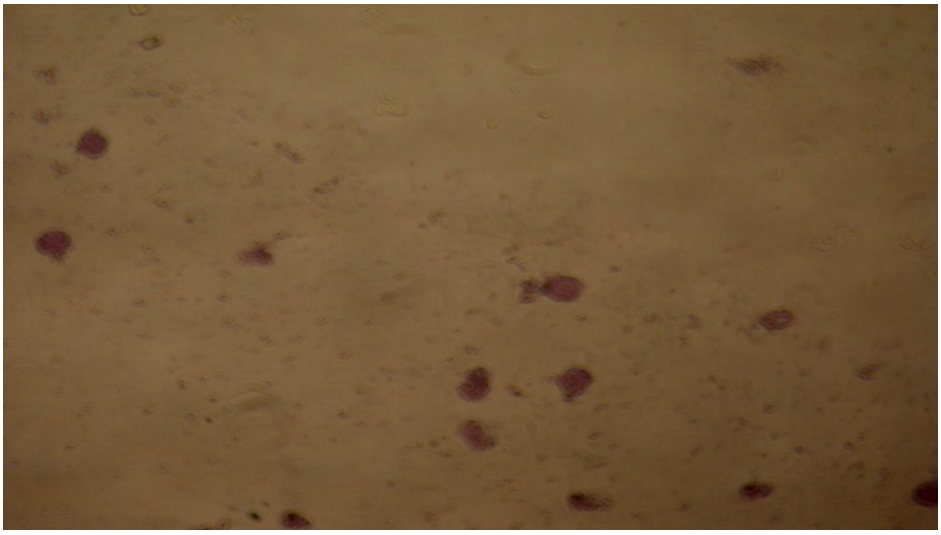

Figure (15): MCF-7 cells treated with Cu(II) complex (2) at 100µg

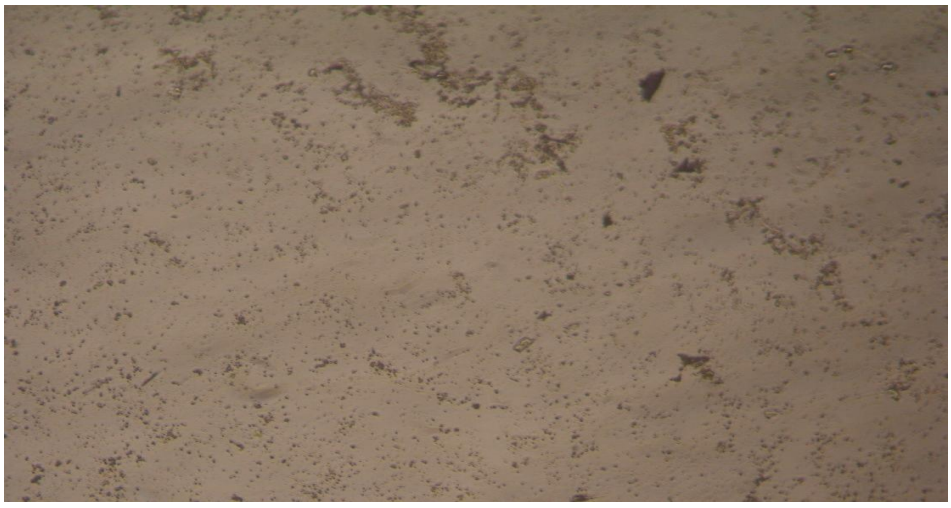

Figure (16): MCF-7 cells treated with Cu(II) complex (2) at 500µg

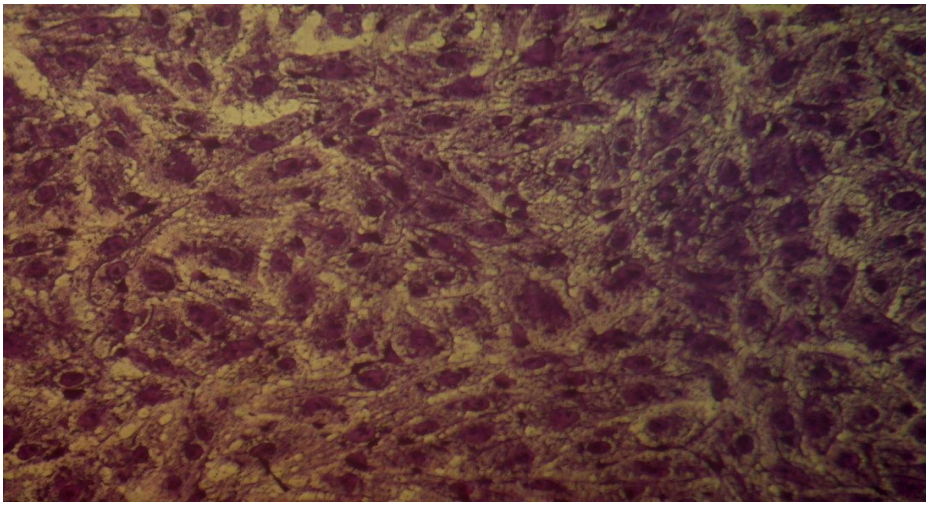

Figure (17): MCF-7 cells treated with Mn(II) complex (3) at 4µg

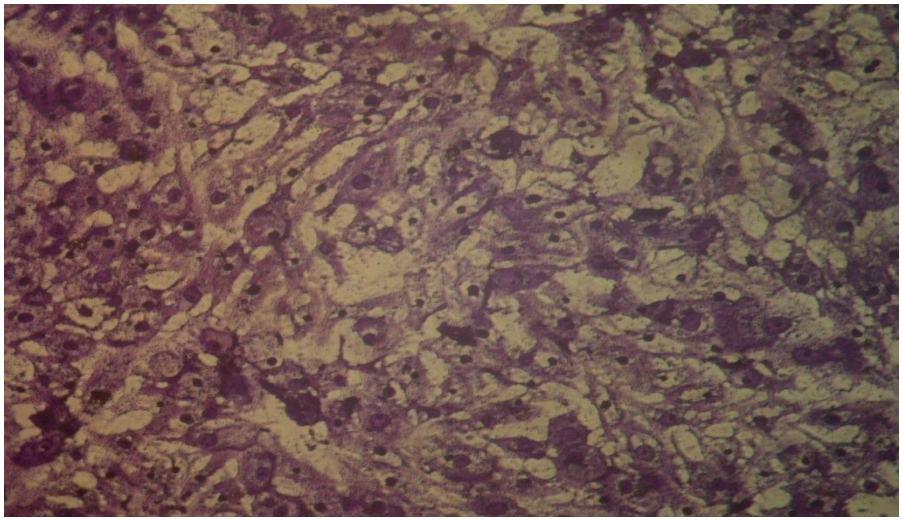

Figure (18): MCF-7 cells treated with Mn(II) complex (3) at 10µg

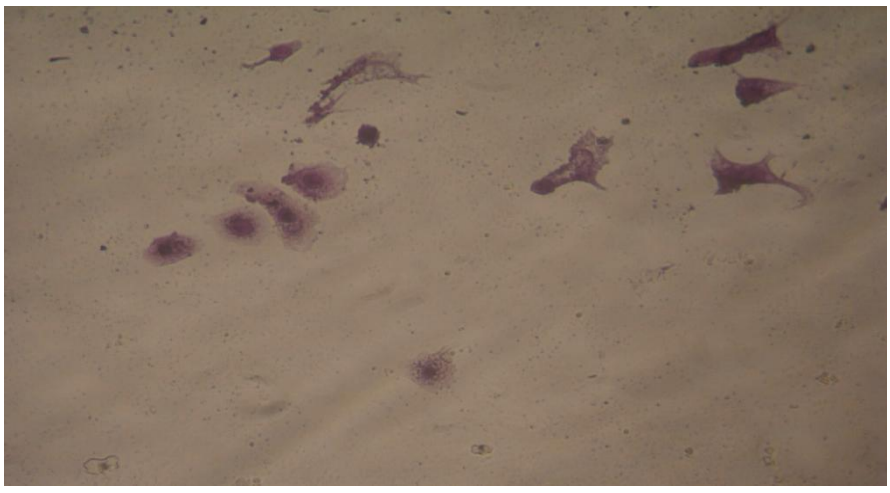

Figure (19): MCF-7 cells treated with Mn(II) complex (3) at 100µg

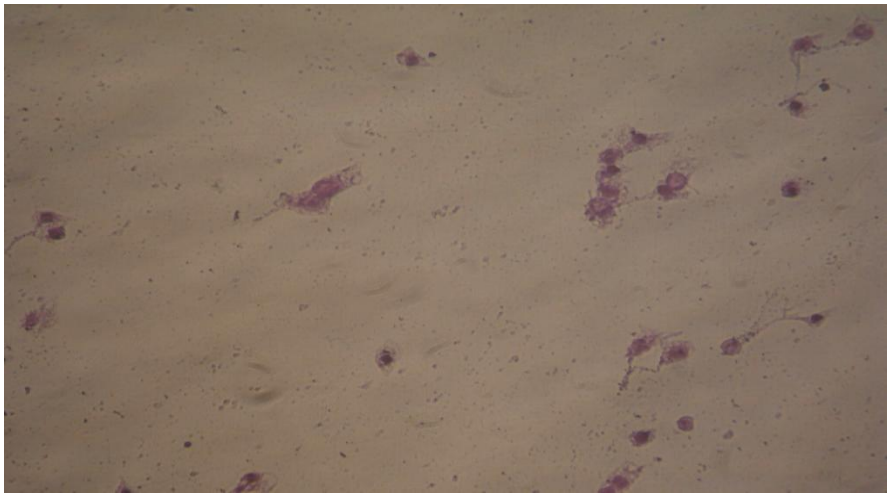

Figure (20): MCF-7 cells treated with Mn(II) complex (3) at 500µg

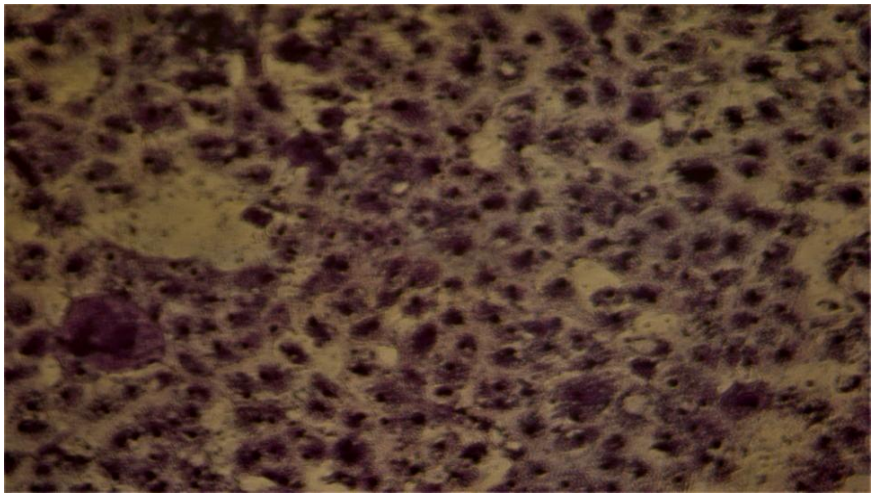

Figure (21): MCF-7 cells treated with Zn(II) complex (4) at 4µg

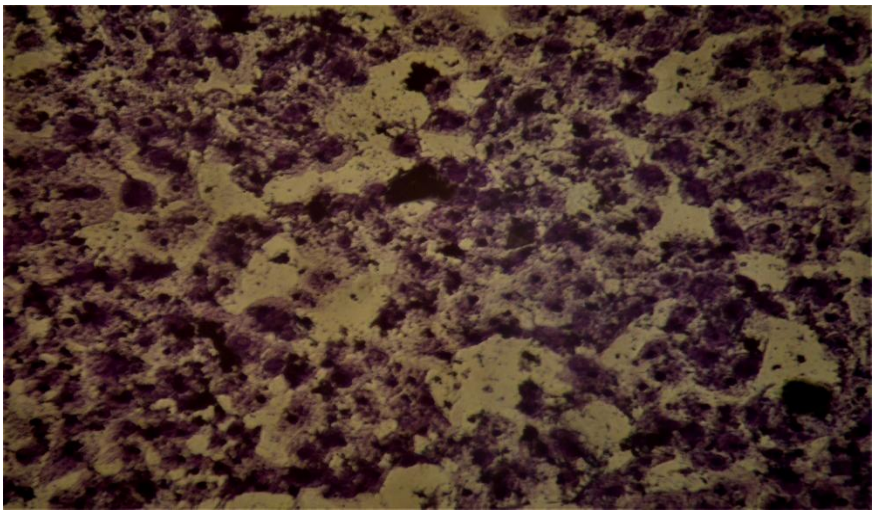

Figure (22): MCF-7 cells treated with Zn(II) complex (4) at 10µg

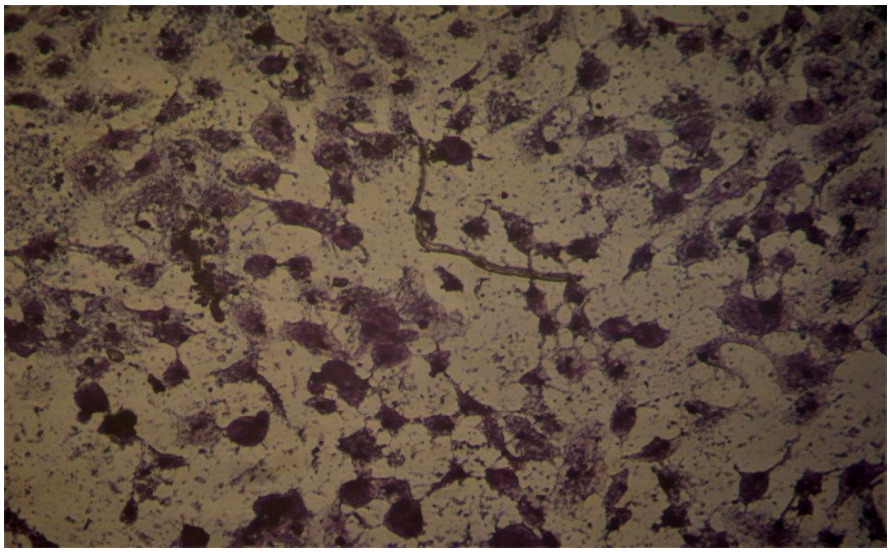

Figure (23): MCF-7 cells treated with Zn(II) complex (4) at 100µg

Figure (24): MCF-7 cells treated with Zn(II) complex (4) at 500µg

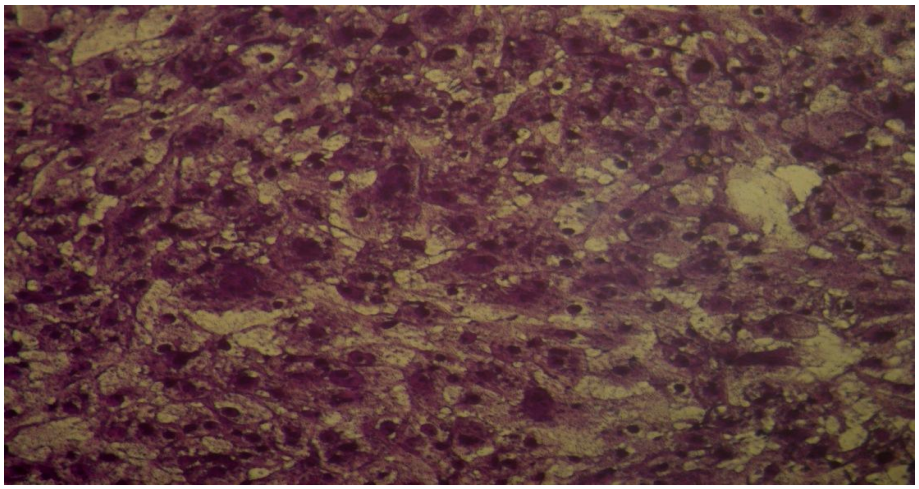

Figure (25): MCF-7 cells treated with Ni(II) complex (5) at 4µg

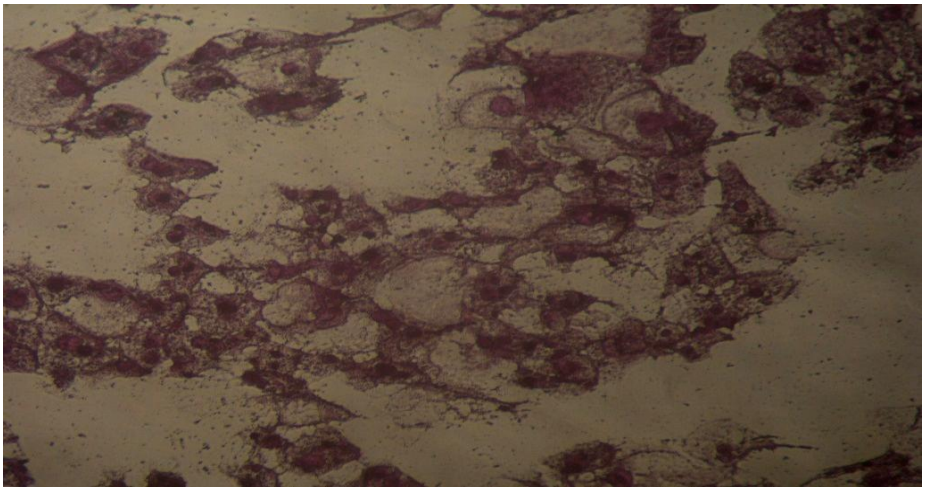

Figure (26): MCF-7 cells treated with Ni(II) complex (5) at at 10µg

Figure (27): MCF-7 cells treated with Ni(II) complex (5) at at 100µg

Figure (28): MCF-7 cells treated with Ni(II) complex (5) at 500µg

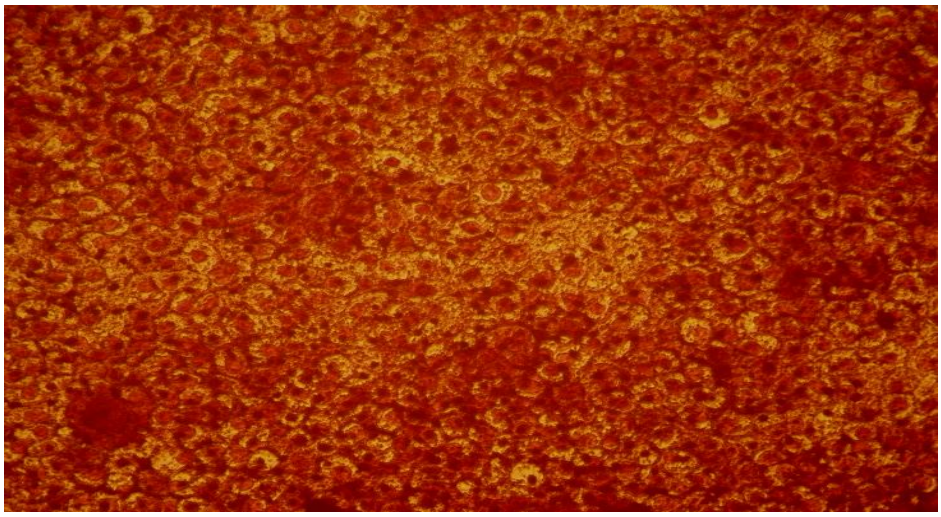

Figure (29): MCF-7 cells treated with Ba (II) complex(15) at 4µg

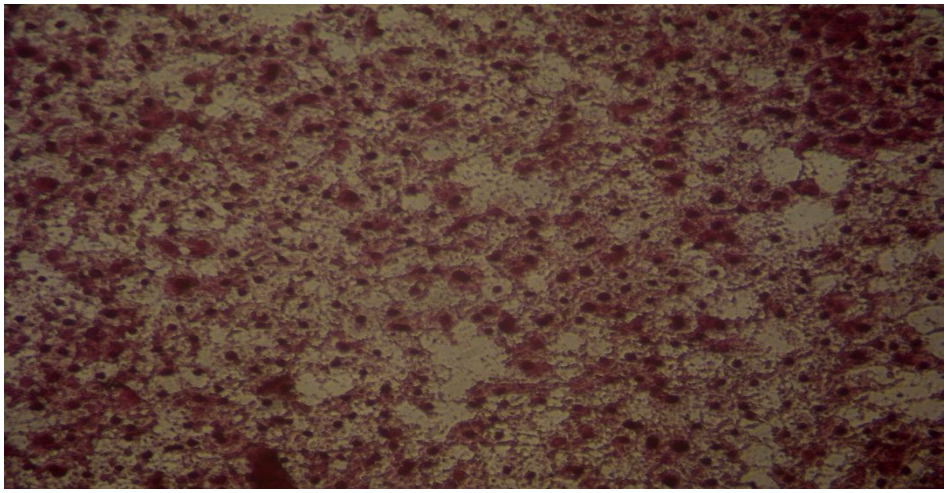

Figure (30): MCF-7 cells treated with Ba (II) complex(15) at 10µg

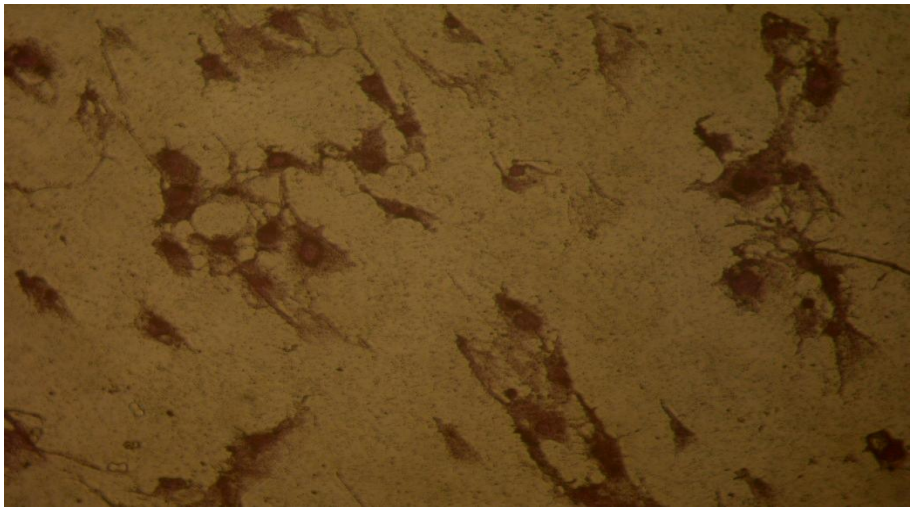

Figure (31): MCF-7 cells treated with Ba (II) complex(15) at 100µg

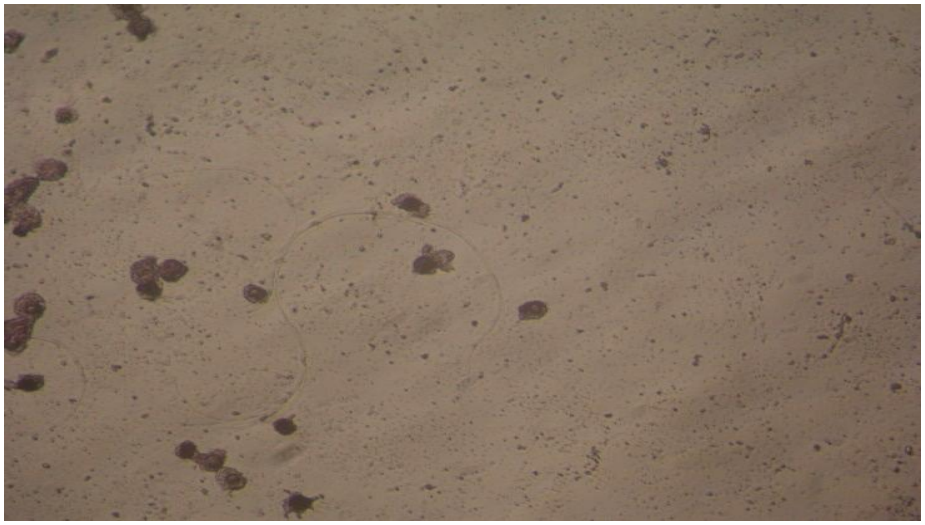

Figure (32): MCF-7 cells treated with Ba (II) complex(15) at 500µg

3.9.2. *Invivo* studies

Determination of liver functions (AST, ALT, and albumin), renal functions (B.Urea & S.Creatinine) and some hematological parameters (Hb, RBCs, TLC and platelets counts) showed no significant differences between treated groups by the chosen complexes and the control group, which proves that there are no toxic side effects for the tested complexes.

Determination of liver function

Table (6): Statistical analysis (ANOVA) for liver function tests in the different groups

Parameters	Control	Complex (2) ($1x10^{-5}$ mmole/L)	Complex (5) ($1x10^{-5}$ mmole/L)
AST (U/l)	**89.40 ± 5.446^{a}**	**98.136 ± 6.02^{bc}**	**99.85 ± 4.34^{bc}**
ALT (U/l)	**50.61 ± 3.88^{a}**	**32.610 ± 3.14^{bc}**	**36.10 ± 6.91^{bc}**
Albumin (g/dl)	**4.02 ± 0.97^{abc}**	**4.17 ± 1.05^{abc}**	**4.11 ± 1.21^{abc}**

ANOVA: analysis of variance, SD: standard deviation; each value is represented as mean ± SD. Data with different superscripts are significantly different at $p \leq 0.05$. [a]Significance versus control group, [b]Significance versus group treated with complex **(5)** with $1x10^{-5}$ mmole/L, [c]Significance versus group treated with complex **(2)** with $2x10^{-5}$ mmole/L

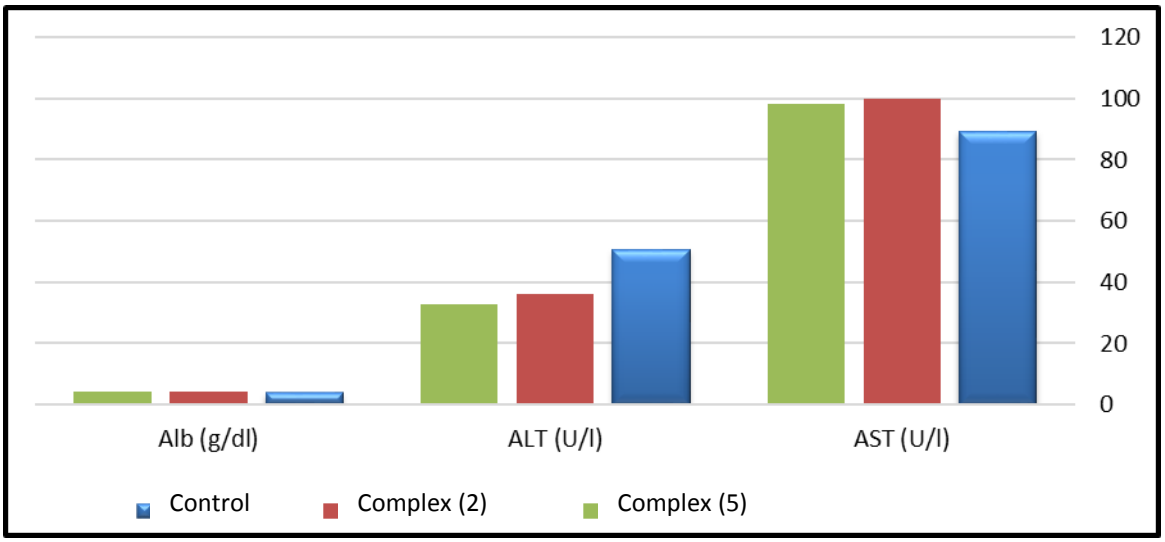

Figure (31): Liver function tests in the different groups

Determination of Renal function

Table (7) : Statistical analysis (ANOVA) for renal function tests in the different groups

Parameters	Control	Complex (2) (1x10-5 mmole/L)	Complex (5) (1x10-5 mmole/L)
B. Urea (mg/dl)	**35.840±3.079^{ac}**	**37.440±2.443^{ac}**	**32.114±2.815^{b}**
S. Creatinine (mg/dl)	**0.585±0.301^{abc}**	**0.571±0.220^{abc}**	**0.520±0.271^{abc}**

ANOVA: analysis of variance, SD: standard deviation; each value represented as mean ± SD. Data with different superscripts are significantly different at $p \leq 0.05$. [a]Significance versus control group, [b]Significance versus group treated with complex **(5)** with $1x10^{-5}$ mmole/L [c]Significance versus group treated with complex **(2)** with $2x10^{-5}$ mmole/L

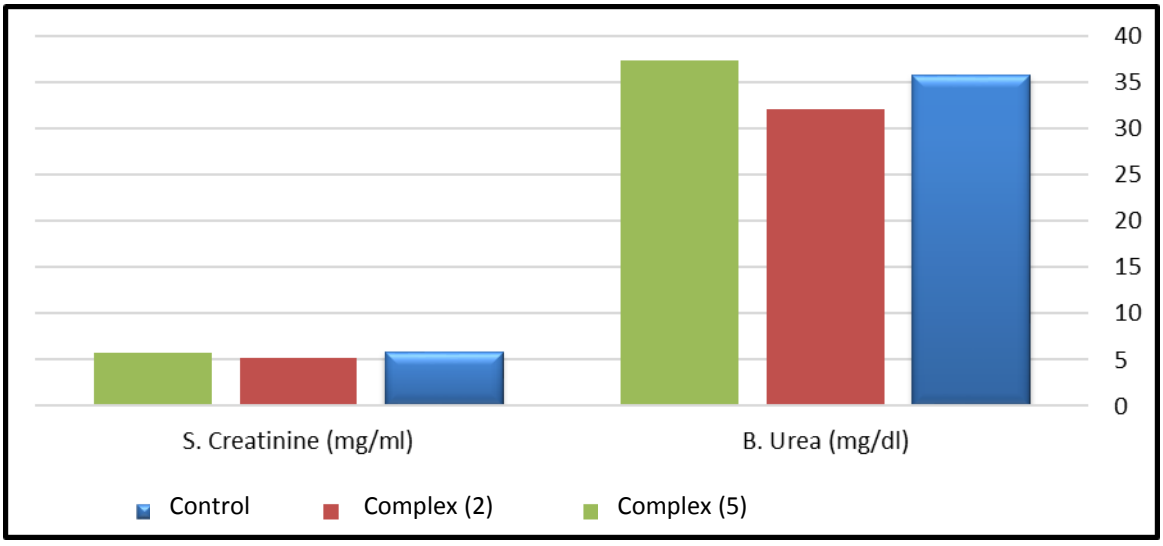

Figure (32): Renal function tests in the different groups

Hematological studies:

Table (8): Statistical analysis (ANOVA) for hematological tests in the different groups

Parameters	Control	Complex (2) ($1x10^{-5}$ mmole/L)	Complex (5) ($1x10^{-5}$ mmole/L)
Hb (g/dl)	**16.020 ± 2.961^{ab}**	**16.20 ± 2.470^{c}**	**15.780 ± 1.890^{ab}**
RBCs (X 10^6/cmm)	**6.471 ± 0.711^{abc}**	**6.237 ± 1.060^{abc}**	**6.121 ± 0.924^{abc}**
TLC (X 10^3/cmm)	**8.911 ± 1.155^{a}**	**9.660 ± 0.980^{bc}**	**10.12 ± 1.917^{bc}**
PLTs (X 10^3/cmm)	**498.142 ± 38.114^{ac}**	**501.081 ± 30.707^{ac}**	**442.991 ± 22.711^{b}**

ANOVA: analysis of variance, SD: standard deviation; each value is represented as mean ± SD. Data with different superscripts are significantly different at $p \leq 0.05$. [a]Significance versus control group, [b]Significance versus group treated by complex**(5)** with $1x10^{-5}$ mmole/L [c]Significance versus group treated by complex **(2)** with $2x10^{-5}$ mmole/L.

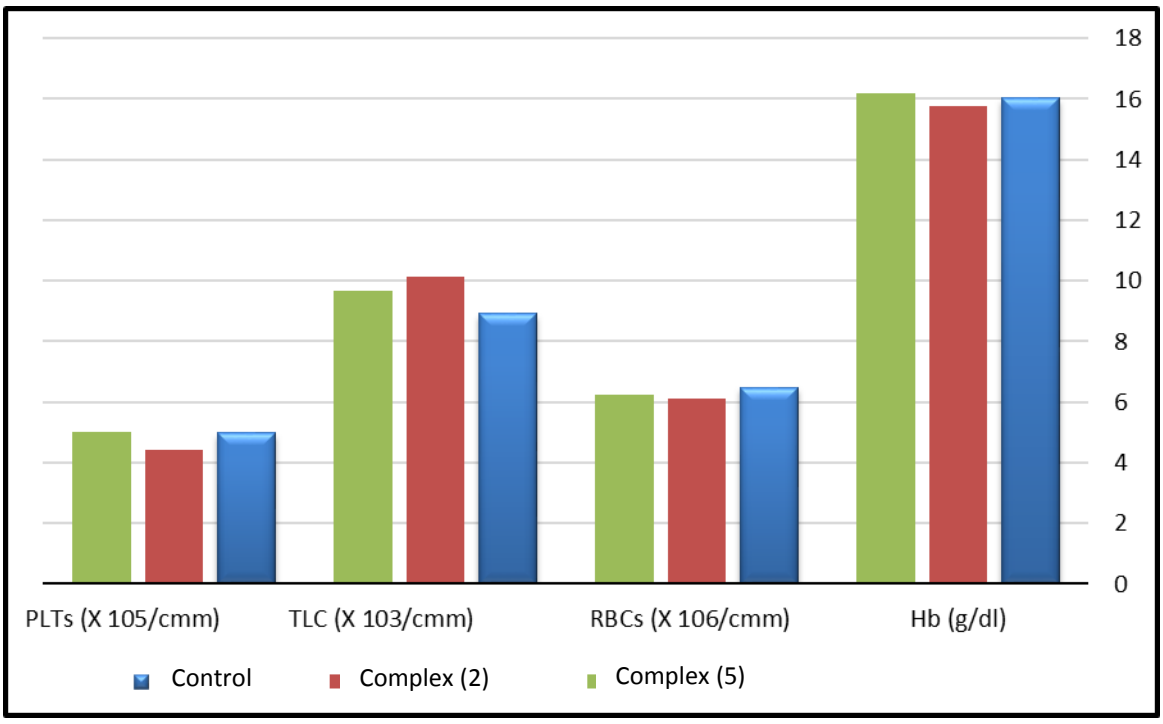

Figure (33): Hematological tests in the different groups

Conclusion

In the present study, new metal complexes were prepared. Structural and spectroscopic properties revealed that, the ligand adopted a tridentate or hexadentate ligand fashion; on the other hand, the metal complexes adopted a

tetragonal distorted octahedral geometry around metal ions. All the complexes are non-electrolytic in nature as suggested by molar conductance measurements. The ligand coordinated to the central metal ion forming five or six membered rings including the metal ions. The antitumor activities of the ligand as well as some of its metal complexes were assessed that, the toxicity of both ligand and metal complexes was found to be concentration dependent, the cell viability decreased with increasing the concentration of complexes.

REFERENCE

1. Umar N, Ndumiso M and Mahmoud. E.S., Metal complexes in cancer therapy an update from drug design perspective. *Drug Des. Devel Ther*., 11: p599-616 (2017).

2. Lian W.T, Wang X.T, Xie C.Z et al., Mixed-ligand cupper schiff-base complexes; The role of the Co-ligand in DNA binding, DNA cleavage, Protein binding and cytotoxicity. *Dalton trans*., 45(22)**:** p9073-9087 (2016).

3. Zou T., Ching Z., Lum T., Lok C.N, Zhang J.J and Che C.M., Chemical biology of anti cancer gold(III) and gold (I) complexes. *Chem.soc.rev*., 44: p8786-8801(2015).

4. Norn S, Permin H, Kruse E. and Kruse PR., Mercury a major agent in the history of medicine and alchemy. *Europe PMC*, 36: p40-41 (2008).

5. El-Tabl A.S, Shakdofa M.M.E, and Wahba M.A. Sugar hydrazone complexes;Synthesis, Spectroscopic characterization and antitumor activity. *Journal of Advan. in Chem.,* 9 (1): p1837-1860 (2014).

6. E l-Tabl A.S, Abdel-Wahed M.M, and Wahba M.A., Synthesis, Characterization and Fungicidal activity of binary and ternary metal(II) complexes derived from 4,4′-4-nitro-1,2-phenylene) bis (azanylylidene))bis(3-(hydroxyimino)pentan-2-one).*Spect.Chimica.*, *Acta* Part A: Molecular and Biomolecular Spectroscopy, 136: p1941-1949 (2015).

7. Netalkar P.P., Netalkar S.P., and Revankar V.K., Transition metal complexes Of Thiosemicarbazone: Synthesis, structures and invitro antimicrobial studies. *Pol.hedrn.*, 100: p 215-222 (2015) .

8. El Bahnasawy R.M., Sharaf El Deen L.M., El Tabl A.S., Wahba M.A and Abdel-Mensef., Electrical conductivity of salicylaldehyde thiosemicarbazone and Pd(II),Cu(II) and Ru(III). *Eur.Chem.Bull,* 3(5) p 441-446. (2014) .

9. Sridevi G., Arul A. S. and Angayarkani R., Schiff base metal complexes as anti cancer agent, *A. J. Chem*., 31(3): 493-504.(2019).

10. Battin S.N., Manikshete A.H., Asabe M.R and Sathe D.J.. Synthesis, Characterization, antimicrobial ,anticancer and anti-hemolatic activity Of Co(II), Ni(II) and Cu(II) complexes with 2-methoxy-6-(3-iminoquinolinly methyl) Phenol. *Advan. Chem.* 7(6)**:** p10-20. (2018)

11. Hossain Md.S., Tariqul H. M., Khan Md. N., Sarker A.Ch., Nasiruddin , Ashraful Alam , Zakaria C.M. and Kudrat Md., A Short Review on Antimicrobial Activity Study on Transition Metal Complexes of Ni Incorporating Schiff Bases. *Bio. Scien.*, 1: 135-145. (2017)

12. Padhye S., Zahra A., and Ekk S. Synthesis and characterization of Copper(II) complexes of 4-alkyl/aryl-1,2-naphthoquinones Thiosemicarbazones derivatives as potent DNA cleaving agents. *Inorg. Chimi. Acta.* 358: p2023– 2030. (2005)

13. Jain S., Sharma A., Agrawal M., Sharma S., Dwivedi J., And Kishore D., Synthesis and Antimicrobial Evaluation of Some Novel Trisubstituted S-Triazine Derivatives Based on Isatinimino, Sulphonamido, and Azacarbazole. *J. Chem.,* Article ID 925439. (2013).

14. Svehla G, Vogel's textbook of macro and semi micro Quantitative inorganic analysis fifth Ed, Longman Inc: New York, (1979).

15. Vogel A, A Text Book of Quantitative Inorganic Analysis, ELBS, London, (1978).

16. Holzbecher Z, Divis L, Kral M, Handbook of organic reagents in inorganic analysis, Handbook of organic reagents in inorganic analysis, John Wiley (1976).

17. El-Tabl A. S., Abd-El Wahed M. M., Ashour A. M., Abu-Setta M. H. H., Hassanein O. H. and Saad A. A., Metallo-organic Copper(II) Complex in

Nano Size as a New Smart Therapeutic Bomb for Hepatocellular Carcinoma. *Journal of Chemistry and Chemical Sciences*; 9(1) p 33-44 . (2019)

18. El-Tabl A. S., Abd-El Wahed M. M, Sayed Ahmed R.A and Sarhan. K S., Synthesis and structural characterization of new and exciting NP complexes-based paracetamol moiety with antimicrobial activity Journal of Chemistry and Chemical Sciences,10(1): p 32-64 , (2020).
19. El-Tabl A. S., Abd-El Wahed M. M, Ashour A.M., and Sayed Ahmed R.A , The new acetaminophen drug in the form of nano-organometallic compounds as a bright future for antimicrobial therapy ,Drug designing open access, 10(2): p 174.(2021).
20. Mazzela F.M., Schumacher H.R.: Hemoglobin. *Clinical Chemistry. Theory. Analysis and Correlation,* 40: p 771-789. (2010).
21. NCCLS document H18-A. Procedures for the handling and processing of blood specimens. National Committee for Clinical Laboratory Standards, Villanova, PA. (1990).
22. Grün B, Zeileis A, Automatic Generation of Exams in R. *Journal of Statistical Software,* 29(10): 1–14. doi:10.18637/jss.v029.i10. (2009).
23. Chaitra, T.K., Mohana K.N.S., and Tandon H.C., Thermodynamic, electrochemical and quantum chemical evaluation of some triazole Schiff bases as mild steel corrosion inhibitors in acid media. *Mole. Liq*., 211: p1026-1038. (2015)
24. Liang, J. Hua and L. Wei and L. Xiao, Synthesis and antibacterial activity of oxime ether non-ketolides, and novel binding mode of alkylides with bacterial RNA. Bio-org. Medic. *Chem. Lett*., 23(5): p 1387-1393. (2013).
25. El Gamal M.I., Mohammed I., Said M., Saadia M and Shehta A., Synthesis and anti-inflammatory activity of novel (substituted) benzylidene acetone oxime ether derivatives: Molecular modeling study. *Eurp. Journ. Medici. Chem*., 45 (4): p 1403 -1414. (2010).
26. El-Tabl A.S., Abdel-Wahed M.M., Aboelazm M.I. and Faheem S.M., Newly Designed Metal-based Complexes and their Cytotoxic Effect on

Hepatocellular Carcinoma, Synthesis and Spectroscopic Studies, *Journ. Chem. Chemic. Scien.,* 10 (1): p10-31. (2020)

27. El-Tabl A.S., Abdel-Wahed M.M., Said R. and Karem S., Synthesis and Structural Characterization of New and Exciting NP Complexes-based Paracetamol Moiety with Antimicrobial Activity, *Journ. Chem. and Chemic. Scien.,* 10(1):p 32-64. (2020).

28. El-Tabl A.S., Gharieb M.M., Hemida H.S. and Faheem S.M., Synthesis, Structural Characterization and Antimicrobial Study on Metal Complexes of New Bioactive Ligand with Terminal Wings, *Journ. Chem. Chemic. Scien.,* 10(2): p 65-85. (2020).

29. El-Tabl A.S., Abdel-Wahed M.M., Nabawy A.A., Faheem S.M., Preparation, Spectroscopy Characterization and Anticancer Activity of New Polyhydroxy Ligand and its Metal Complexes, *Journ. Chem. and Chemic. Scien.,*10(5): p 230-252. (2020).

30. El-Tabl A.S., Abdel-Wahed M.M., and Hashim S.M.F., Metal Chelates as Antitumor Agents: Synthesis, Spectroscopic Characterization and Cytotoxic Action of Metal Chelates of New Dioxime Ligand, *Journ. Chem. and Chemic. Scien.,* 8 (8):p 1026-1047. (2018).

31. El-Tabl A.S., Abdel-Wahed M.M., Wahba M.A. , Elgamasy S.M. and Nabawy A.A., Synthesis, Spectroscopic Characterization and Cytotoxic Activity of New Metal Complexes with Novel Hydrazononaphthalenol Ligand Against A-549 Cell Line, *Journ. Chem. and Chemic. Scien.,* 6(4): p 293-307. (2016).

32. El-Tabl A.S., Abdel-Wahed M.M., Wahba M.A., Synthesis of novel metal complexes with isonicotinoyl hydrazide and their antibacterial activity. *Journ. Chemic. Res*., 34(2): p 88-91. (2010).

33. El-Tabl A.S., Novel N,N-diacetyloximo-1,3-phenylenediamine copper (II) complexes *Trans. Meta. Chem*., 22(4) p 400-405. (1997).

34. El-Reash, Ibrahim K.M., and Bekheit M.M., Ligational behaviour of biacetylmonoxime nicotinoyl hydrazone (H_2BMNH) towards transition metal ions. *Trans. Meta. Chem*., 15 (2): p 148-151. (1990) .

35. Chaudhary N.K. and Mishra P.. Metal Complexes of Novel Schiff Base Based on Penicillin: Characterization, Molecular Modeling, and Antibacterial Activity Study. *Bioinog. Chem. App*., ID 6927675. (2017).

36. Lever A., Electronic spectra of some transition metal complexes: Derivation of Dq and B. *Journ. Chemic. Education*, 45(11)**:** 711. (1968).

37. El-Tabl A.S., Abdel-Wahed M.M., Abdelrazek S.E., Dabrowska A.M. and Elgamasy S.M.; Antibactrial evaluation of ethoxy-omix schiff base ligand and its Metal Complexes. *Asian Journ. Scien. Tech*. 7(7): p 3167-3180. (2011).

38. El-Tabl A.S., Abdel-Wahed M.M., Rezk A., *Spect. chimi. Acta* - Part A: Molecular and Biomolecular Spectroscopy 117:p772–788.(2014).

39. Aslan H.G., Özcan S., and Karacan N., Synthesis, characterization and antimicrobial activity of salicylaldehyde benzenesulfonyl hydrazone and its Nickel (II), Palladium (II), Platinum (II), Copper (II), Cobalt (II) complexes. *Inorg.Chem.Commu.*, 14(9)**:** p 1550-1553. (2011).

40. Mohamed G.G., Omar M., and Hindy A.M., Synthesis, characterization and biological activity of some transition metals with Schiff base derived from 2-thiophene carboxaldehyde and aminobenzoic acid. *Spect. Chimic. Acta* Part A: Molecular and Biomolecular Spectroscopy, 62 (4)**:** p 1140-1150. (2005).

41. Geary W.J., The use of conductivity measurements in organic solvents for the characterisation of coordination compounds. *Coord. Chem. Rev*., **7**(1): p 81-122. (1971).

42. El-Tabl A.S., Shakdofa M.M.E., Herasha B.M., Antibacterial activities and spectroscopic characterization of synthetic metal complexes of 4-(3- (hydroxyimino)-4-oxopentan-2-ylidene) amino)-1,5- dimethyl-2-phenyl-1H-pyrazol-3(2H)-one. *Main Group Chemistry* 12(3)**:**p 257–274. (2013).

43. El-Tabl A.S., Abdel-Wahed M.M.; Wahba M.A., Synthesis, spectroscopic investigation and biological activity of metal (II)

complexes with N_2O_4 ligands. *Journal of Chemical Research*, (9): p 582-587. (2009).

44. El-Tabl A.S., Abdel-Wahed M.M., Mohammed M.H., Synthesis, spectral characterisation and cytotoxic effect of metal complexes of 2-(2-(4- carboxyphenyl)guanidino) acetic acid ligand. *Chem. Spec. Bioavaib*., 25 (2):p 133 -146. (2013).

45. El-Tabl A.S., Abdel-Wahed M.M., El-Assaly M.M, Ashour A.M. Nano organo metallic complexes as therapeutic platforms against breast cancer cell lines; (*invitro* study), *Egy. Journ. Chem*.,64 (3):p 10-21. (2021).

46. El-Tabl A.S., Abdel-Wahed M.M., Stephanos J.J., El-Gamasy S.M . Novel metal complexes of guanidine ligand; synthesis, spectroscopic characterization and biological activity. *Intern. Journ. Chem. Tech*. Res. 5 (1): p 430 – 449. (2013).

47. El-Tabl A.S., Shakdofa M.M., Elseidy A.M . Synthesis, characterization and ESR studies of new copper(II) complexes of vicinal oxime ligands *Journal of Kor. Chem. Soc*. 55 (4): p 603 - 611. (2011).

48. El-Tabl A.S., Elsaied A. and Alhakimi A.N. Synthesis, spectroscopic investigation and biological activity of metal complexes with ONO trifunctionalizedhydrazone ligand, *Trans.Met.Chem*.,32:p689-701(2007).

49. Surati K.R. Synthesis, spectroscopy and biological investigations of manganese (III) Schiff base complexes derived from heterocyclic β-diketone with various primary amine and 2, 2′-bipyridyl. Spect.*Chimic. Acta* Part A: Molecular and Biomolecular Spectroscopy, 79(1): p 272-277. (2011)

50. El-Tabl, A.S., Abd-Elzaher F.A., Shakdofa M M., E.Rasras M.M., Anas J.., Synthesis, physicochemical studies and biological evaluation of unimetallic and heterobimetallic complexes of hexadentatedihydrazone ligands.Beni-Suef University Journal of Basic and Applied Sciences,. 6(1): p. 24-32(2017).

51. El-Tabl, A.S., et al., Synthesis, structural characterization, electrochemical and biological studies on

divalent metal chelates of a new ligand derived from pharmaceutical preservative, dehydroacetic acid, with 1, 4-diaminobenzene. *Arabian Journal of Chemistry*,. 10: p. S3816-S3825 (2017).

52. El-Tabl, A.S., Abd-El Wahed M .M., and Abu-Setta M.H.H., METALLO-BIOACTIVE COMPOUNDS AS POTENTIAL NOVEL ANTICANCER THERAPY. *Journal of Chemistry and Chemical Sciences* (2015).
53. El-Tabl A, S,., et al., Synthesis, Structural Characterization and Study of Some New Antimicrobial Action of Metal Complexes of (E)-N', N''-bis ((Z)-4-fluorobenzylidene)-2- (naphthalen-1-yloxy) acetohydrazono-hydrazide Schiff Base. *Journal of Chemistry and Chemical Sciences*,. 6 (6): p. 513-536 (2016).
54. Ali A., Akbar M. and Paul V. Mixed-ligand ternary complexes of potentially pentadentate but functionally tridentate Schiff base chelates. *Pol.hed.*, 30(3): p 542-548. (2011).
55. El-Tabl A.S., Abdel-Wahed M.M., Wahba M.A. Synthesis of novel metal complexes with isonicotinoyl hydrazide and their antibacterial activity. *Journ. Chem. Res*., 34(2): p 88-91. (2010).
56. El-Tabl A.S and Ayad M.I. ESR studies on copper(II) complexes of 1,3diamonopropane and 1,2-diaminopropane , *Polish. J. Chem*.,72: p 263-269. (1999).
57. Xia L., Fen Yu. and Huang. Benzaldehyde Schiff bases regulation to the metabolism, hemolysis, and virulence genes expression in vitro and their structure–microbicidalactivity relationship. *Eur. Journ. Med. Chem*.,97: p 83-93. (2015)
58. Smith, D., Chlorocuprates(II).*Coord. Chem. Rev*., 21(2)**:** p 93-158. (1976).
59. Kivelson D., and Neiman R., ESR studies on the bonding in copper complexes. *The Journ. Chem. Phys*., 35(1)**:** p 149-155. (1961).

60. El-Tabl A.S., Wahba M,A., El-Assaly S., Saad A.L., Sugar Hydrazone Complexes; Synthesis, Spectroscopic Characterization and Antitumor Activity. *Journ. Advan. Chem.* , 9(1): p 1837-1860. (2014).

61. Al-Zoubi W, Kandil F and Chebani M.K., Synthesis of macrocyclic schiff bases based on pyridine-2, 6-dicarbohydrazide and their use in metal cations extraction, *Organic Chem Current Res*., 1(1): p 1-7. (2012)

62. Avaji P.G., Patil S.A., and Badami P.S., Synthesis, spectral, thermal, solid-state DC electrical conductivity and biological studies of Co(II) complexes with Schiff bases derived from 3-substituted-4-amino-5-hydrazino-1, 2, 4-triazole and substituted salicylaldehydes,*Trans. Met. Chem.*, 33: p 275-283. (2008).

63. El-Tabl A.S., Abdel-Wahed M.M., Organic amino acids chelates; preparation, spectroscopic characterization and applications as foliar fertilizers. *Journ. Advan. Chem*., 10(2): p 2203-2217. (2014).

64. Mitu, Ilis L., Raman M., Imran N., And Ravichandran S., Transition metal complexes isonicotinoyl hydrazone-4-diphenylaminobenzaldehyde: Synthesis, characterization and antiumer studies. *Eur.Journ. Chem*.,9(1)**:** p 365-372. (2012).

65. Suvarapu L.N., Seo Y.K., Okbaek S. and Ammireddy V.R., Review on Analytical and Biological applications of Hydrazones and their Metal Complexes. *Journ. Chem*.9(3): p 1288-1304. (2012).

66. Qi G.F., Yang Z.Y., and Qin D.D., Synthesis, characterization and DNA binding properties of the Cu(II) complex with 7-methoxychromone-3-carbaldehyde-benzoyl hydrazone, *Chem. Pharma. Bull*., 57: p 69-73(2009)

67. Opletalová V., Kalinowski D.S., Vejsová M., Kuneš J.I., Pour M., Jampílek J., Identification and characterization of thiosemicarbazones with antifungal and antitumor effects: cellular iron chelation mediating cytotoxic activity," *Chem. Res. Toxic*., 21: p 1878-1889 . (2008).

68. El-Tabl A.S., Shakdofa M.M., and ElseidyA., Synthesis, Characterization and ESR Studies of New Copper(II) Complexes of Vicinal Oxime Ligands, *Journ.. Kor. Chem. Soc*., 55:p 603-611. (2011)

69. Lima L.M., Frattani F.S., Dos Santos J.L., Castro H.C., Fraga C.A.M and Zingali R.B., Synthesis and anti-platelet activity of novel arylsulfonate–acylhydrazone derivatives, designed as antithrombotic candidates, *Eur. Journ. Med. Chem*., 43: p 348-356. (2008)

70. Bernhardt P.V., Mattsson J., and Richardson D.R., Complexes of cytotoxic chelators from the dipyridyl ketone isonicotinoyl hydrazone analogues, *Inorg. Chem*., 232 (45): p752-760. (2006).

71. Green D.A., Antholine W.E., Wong S.J., Richardson D.R and Chitambar C.R., Inhibition of Malignant Cell Growth by 311, a Novel Iron Chelator of the Pyridoxal Isonicotinoyl Hydrazone Class Effect on the R2 subunit of Ribonucleotide Reductase, *Clinc. Canc. Res*., 7: p 3574-3579. (2001).

72. El-Tabl A.S., Shakdofa M.M and Elseidy A., Synthesis, Characterization and ESR Studies of New Copper(II) Complexes of Vicinal Oxime Ligands, *Journ. Kor. Chem. Soc*., 55: p 603-611. (2011)

73. El-Tabl A.S., Abdel-Wahed M.M., Elbasyouny M.M., and Faheem S.M., Preparation, Spectroscopic Characterization and Antitumor Activity of New Metal Complexes of Sodium 4,4'- ((2E,2'E)-2,2'- ((4,6-dihydroxy-1,3-phenylene) bis (ethan-1-yl-1-ylidene)) bishydrazinecarbonyl)) diphenolate hydrate, *Journ. Chem. Chemic. Scien*., 10(5)**:** p 177-200. (2020)

74. El-TablA.S., Abdel-Wahed M.M and El-Saied A., Design, Spectroscopic Charactarization and Antitumor Action of Synthetic Metal Complexes of Novel Benzohydrazide Oxime. *Journ. Chem. Chemic. Scien.*, 8(8): p 1048- 1072. (2018).

Corresponding author : **Mohammed H. H. Abu-Setta**

Department of Chemistry, Faculty of Science, El-Menoufia University, Shebin El- Kom, Egypt.

Email: **drmohammedhosnyabusetta@gmail.com**